Response to 2nd comments of reviewers

2nd review of "The optical, physical properties and direct radiative forcing of urban columnar aerosols in Yangtze River Delta, China" by Zhuang et al.

The revised manuscript improves the quality to some extent. However it is still unnecessarily lengthy, it is not well presented, and there are many unjustified or weakly justified statements/conclusions; the language is poor and there are numerous grammatical errors. Further revision is required before it is considered for publication.

Dear reviewer

Thanks again for reviewing our manuscript and providing us significant comments and suggestions. In view of the above-mentioned issues, the manuscript has been further shortened (by about 12%, ~1200 words) and re-edited in English by Wiley Editing Services (Certificate is attached below). Additionally, the authors further confirm the statements and conclusions in the manuscript to avoid imprecisely. We will response to your comments carefully point by point; details of the revisions can be referred to the new version of the manuscript.

Relevant changes of the revised manuscript (marked with traces) are enclosed in the last part of this document.

There are many places need to be revised for these issues, and in the following I just name a few as examples.

1. Abstract. The abstract should be a condensed version of the conclusion. When I go through the Abstract and the Conclusion, I find many inconsistencies in between. For example, with regarding the aerosol DRF, when the abstract focuses fine aerosol DRF, the conclusion focuses the total aerosol DRF; when the abstract deals with the coarse/fine fractions (15%, 51%), the abstract deals with coarse/total quantities (14%, 34%).

R: Thank you for your reminding.

To make the Abstract and the Conclusions consistency in between, the Conclusions has been rephrased accordingly in revised manuscript. Additionally, the corresponding descriptions in Section 3 have also been changed to keep in consistency in full text.

2. Ls 213-214: "The table also implies that west YRD could suffer very serious particle pollutions". I don't understand how this statement/conclusion can be made based solely on Table 1. Also, Ls 236-237, "the seasonal variations of its fine and coarse AEs are well agree with each

other". This is not true for scattering aerosols and total aerosols.

R: Thank you for figuring out the confusing statements in the manuscript.

We agree with you that the statement in Ls213-214 is not rigorous based solely on Table 1, although the maximal AOD in the table shows extremely large value. This sentence has been deleted in revised manuscript.

The sentence in Ls236-237 was tried to describe a consistent or opposite variations between the fine and coarse AEs' seasonality for each aerosol type; because their linear correlation coefficient is considerably large (0.84 for scattering aerosol and 0.97 for absorbing aerosol). To make it more clearly, the sentence has been rephrased.

3. Seasonal variation of aerosol optical properties. The authors claim that the aerosol optical properties have "substantial seasonal variations". This is not true for AOD. Based on Figure 1(a) and (b), there are not evident seasonal variations for total AOD and total SAOD. For AOD, one standing-out result as shown in Fig 1 is that the AOD in August is "unusually" high ("unusually" here means compared to the neighboring months, even throughout the entire year). This is an interesting result, and the authors should examine why.

R: Thank you for your question. With respect to the total AOD and total SAOD, Ls224-226 (in original version) has stated that AODs of the total aerosol and the total scattering aerosol had weaker seasonality than those of the fine or coarse aerosols. And the possible explanations have also been carried out accordingly. In revised manuscript, the statements on the aerosol variations have been checked or rephrased throughout the whole text to make them more justified and clearly.

AOD values in August have been checked before they are used and analyzed.

As mentioned in Methodologies, the data from May to Sep 2012 and from Aug to Dec 2013 were invalid or missed due to the malfunctions of the instrument and the problems of data transmission. Thus, the August AODs in 2012 and 2013 were not included in this study. Coincidentally, air pollution has started to be controlled since 2012 in Nanjing due to hosting international events in Aug 2013 (Asian Youth Games) and 2014 (Youth Olympic Games). And the aerosol loadings were relatively lower in August 2012 and 2013, which could be reflected from MODIS retrievals. The MODIS AOD in August in urNJ was 1.18 in 2011 while was 0.75 and 0.63 in 2012 and 2013, respectively. MODIS products also show that the July AODs were all smaller than the August

ones in these three years. As a result, the AOD in August shown in Figure 1 is “unusually” high. Corresponding statement has been included in the revised manuscript.

4. L259, “SSA is the smallest in spring”. This is not true either. Based on Fig 3, SSA is lowest in July and September, and if the August data point is not considered, SSA is lowest in the summer. Again, I strongly suggest the authors to examine the August data and results, which may have important influences on some results and conclusions of this study, and it could be an important finding too.

R: Thank you for figuring out the imprecise expression here.

As mentioned previously, data in August has been checked. Large SSA in August is mainly derived from a higher scattering fraction of the aerosols.

And we agree with you that SSA is small in July and September, however, the seasonal mean SSA of the total aerosols in spring (MAM) is a little smaller than in summer (JJA) no matter including (Table 3) or excluding the August value. The mean SSA in spring is still 0.002 smaller than in summer when excluding August SSA. The confusing statement in L259 has been rephrased in revised manuscript.

5. Ls 318-319 and Fig 5, “AOD observed by CE-318 are in “reasonable agreement with those from MODIS in seasonal variation and magnitude”. I don’t know what the “reasonable agreement” means here. In fact, if ignoring the highest AOD data point, the MODIS AOD is about twice of the CE-318 AOD. I guess the highest AOD value is the AOD in August, and if so, the August data plays a big role.

R: Thank you for your question and comment.

The sentence in Ls318-319 was tried to describe a relatively well relationship between the MODIS and CE-318 AODs and AEs. This sentence has been rephrased to make it more clearly.

Indeed, the seasonal mean MODIS AODs are mostly larger than the CE-318 ones in urNJ, which is similar to that in central China (Dong et al., 2013). However, I’m afraid we could not agree with you that the MODIS AOD is almost twice of the CE-318 AOD. MODIS AOD is about 1.2 times of the CE-318 AOD during the study period, no matter including or excluding the August AODs.

Some modifications have been made to this part, in which Fig. 5 has been redrawn in revised manuscript. Because the seasonal mean values of MODIS products in Fig. 5 (original version) include the results in the maintaining periods of CE-318. In update Fig. 5, the monthly mean AODs and AEs were used to substitute their seasonal mean values to better present the relationship between the MODIS and CE-318 aerosol optical properties. And the slope of the linear fitting in new figure is 1.12 for AOD, similar to that in central China (1.16, Dong et al., 2013).

Reference:

Dong, Z. P., Li, X. M., Du, C. L., and, Zhang, G. J.: Study on aerosol optical property in Xi'An Region, Plateau Meteorology, 32(3), 856-864, doi:10.7522/j.issn.1000-0534.2012.00079, 2013.

6. DRF in Table 3. Why the total DRF is not the sum of the contributions from the fine and coarse aerosols for all aerosol components (total, scattering, absorbing)? Explanations are needed.

R: Thank you for your question.

The coarse aerosol affection on the solar radiation is excluded when calculating the fine aerosol DRF individually, and vice versa. Therefore, the total DRF in Table 3 is not exactly the sum of the contributions from the fine and coarse aerosols. Similarly, the total aerosol RF is also not the sum of the contributions from the aerosol direct and indirect RFs if the latter two DRFs were investigated separately. As indicated in Wang et al. (2010), the simulated direct, indirect and total effect RF of nitrate aerosol is about -0.88, -2.47 and -2.52 W/m^2, respectively. Corresponding explanations have been included in the revised manuscript.

Reference:

Wang, T., Li, S., Shen, Y., Deng, J., and Xie, M.: Investigations on direct and indirect effect of nitrate on temperature and precipitation in China using a regional climate chemistry modeling system, J. Geophys. Res., 115, D00K26, doi:10.1029/2009JD013264, 2010.

7. Sect 3.1.4, many redundancies as in the Introduction.

R: Thank you for pointing out the redundancies.

The revised manuscript has been shortened necessarily and significantly, by 12.3% (~1200 words) for the whole text. The shortened parts are mainly in Section 3 (**Results and discussions**, by 15.8%, ~1029 words) and Section 1 (**Introduction**, by 10.8%, ~160 words). Details can be found in the track version of the revised manuscript.

8. Etc., etc.,…

R: Based on your comments, we have carefully addressed the issues concerned throughout the whole manuscript, including shortening the unnecessary texts, identifying the statements and conclusions and re-editing the languages, to make the revised manuscript being better presented and suitable for publication.

LANGUAGE EDITING

CERTIFICATE

This document certifies that the manuscript listed below was edited for proper English language, grammar, punctuation, spelling, and overall style by one or more of the highly qualified native English speaking editors at Wiley Editing Services.

Manuscript title:

The optical, physical properties and direct radiative forcing of urban columnar aerosols in Yangtze River Delta, China

Authors:

Bingliang Zhuang, Tijian Wang1, Jane. Liu, Huizheng Che, Yong Han, Yu Fu, Shu Li, Min Xie, Mengmeng Li, Pulong Chen, Huimin Chen, Xiu-qun Yang, Jianning Sun

Date Issued:

November 10, 2017

Certificate Verification Key:

CF05-5648-2836-B130-3B7P

This certificate may be verified at https://secure.wileyeditingservices.com/certificate. This document certifies that the manuscript listed above was edited for proper English language, grammar, punctuation, spelling, and overall style. Neither the research content nor the authors' intentions were altered in any way during the editing process. Documents receiving this certification should be English-ready for publication; however, the author has the ability to accept or reject our suggestions and changes. If you have any questions or concerns about this document or certification, please contact help@wileyeditingservices.com.

The optical properties, physical properties and direct radiative forcing of urban columnar aerosols in the Yangtze River Delta, China

Bingliang Zhuang[1, *], Tijian Wang[1, **], Jane. Liu[1,2], Huizheng Che[3], Yong Han[1], Yu Fu[4], Shu Li[1], Min Xie[1], Mengmeng Li[1], Pulong Chen[1], Huimin Chen[1], Xiu-qun Yang[1], Jianning Sun[1]

[1] School of Atmospheric Sciences, CMA-NJU Joint Laboratory for Climate Prediction Studies, Jiangsu Collaborative Innovation Center for Climate Change, Nanjing University, Nanjing 210023, China

[2] Department of Geography and Planning, University of Toronto, Toronto, M5S 3G3, Canada

[3] Key Laboratory of Atmospheric Chemistry (LAC), Chinese Academy of Meteorological Sciences (CAMS), CMA, Beijing, 100081, China

[4] Dalian Weather Modification Office, Dalian, 116001, China

[*] Corresponding author, E-mail: blzhuang@nju.edu.cn; Tel.: +862589681156; ~~fax~~Fax: +862589683797

[* *]Corresponding author, E-mail: tjwang@nju.edu.cn; Tel.: +862589683797; ~~fax~~Fax: +862589683797

Abstract: The ~~fractionated aerosol~~ optical and physical properties ~~of fractionated aerosols~~ as well as ~~their associatedits~~ the direct radiative forcings (DRF) of fractionated aerosols in the urban area of the western Yangtze River Delta (YRD) are investigated ~~usingwith, based on the~~ measurements from a~~of~~ Cimel sun--photometer combined with a radiation transfer model. Ground--based observations of~~ed~~ aerosols have much higher temporal resolutions than ~~those of compared with~~ satellite retrievals. An initial a~~A~~nalysis ~~firstly~~ reveals the characteristics of the optical properties of different types of fractionated aerosols ~~optical properties of different aerosol types~~ in western YRD. The ~~annual mean optical depth of the~~ total aerosols ~~is 0.65±0.28~~, mostly composed~~which is dominated~~ by ~~the~~ scattering ~~aerosols~~ components (93.8%), ~~that~~ have a~~with a~~ mean optical depth of 0.65 at 550nm and refractive

index of 1.44+0.0084i at 440 nm. The fine aerosols are ~~about 4~~approximately 4 times more abundant ~~to, and also~~ and have very different compositions from ~~the~~ coarse aerosols~~ones~~. The absorbing components ~~only~~ account for only ~4.6% of~~in~~ fine aerosols and~~while~~ 15.5% of~~in~~ coarse aerosols and~~, but within the same mode, they~~ have smaller sizes than the scattering aerosols within the same mode. Therefore, ~~the~~ fine particles have stronger~~are much~~ scattering than ~~the~~ coarse ones, simultaneously reflecting the ~~that each component has~~ different size distributions between the absorbing and scattering aerosols. The r~~R~~elationships among the optical properties quantify the aerosol mixings and~~d they~~ imply that ~~about 1~~approximately 15% and 27.5% of the total occurrences result in~~of~~ dust and black carbon dominating~~ed~~ mixing aerosols, respectively, in the western YRD. ~~Differingent from~~ Unlike the optical properties, the size distributions of aerosols in the western YRD ~~have the~~ are similar ~~volume size distributions~~ to those found ate ~~ones in~~ other sites over eastern China on a climatological scale~~ly~~, peaking at ~~the~~ radi~~us~~ of 0.148 and 2.94 μm. ~~But~~ However, further analysis ~~further~~ reveals that the ~~fine- or~~ coarse--dominated particles can~~ould~~ ~~individually~~ also lead to severe haze pollution~~s~~ over the~~in~~ YRD. Observation--~~ed based e~~based estimations indicate that both ~~the~~ fine and coarse aerosols in the western YRD exert a negative DRF, ~~although~~and this is especially true for fine aerosols~~, especially for the former one~~ (-11.17 W/m^2 at the top of atmosphere, TOA). A higher absorption fraction ~~directly~~ leads directly to the negative DRF being further offset ~~more substantially~~ for coarse aerosols (-0.33 W/m^2) at the TOA. Similarly, the coarse mode DRF ~~only~~ contributes to only ~~-14~~13.3% of the total~~within~~ scattering aerosols but~~while~~ >~~34~~33.7% to the total ~~witnin~~ absorbing aerosols. Sensitivity~~e~~ analysis states that aerosol DRFs are~~is~~ not highly~~very~~ sensitive to ~~its~~ their profiles in clear--sky conditions. ~~Both~~ Most of the aerosol properties and DRFs have substantial seasonality in the western YR~~D. ResultsD~~. The results further reveal the contributions of each component of the~~in~~ different size particles~~segments~~

to the total aerosol optical depths (AODs)~~AODs~~ and DRFs. ~~Also,~~Additionally, these results~~y~~ can be used to~~are advantageous to~~ improve aerosol ~~the~~ modelling performance~~s on the aerosol~~ and the modelling of aerosol~~its~~ effects in the eastern regions of China.

1 Introduction

Atmospheric aerosols have significant influences on air quality, human health, and regional/global climate changes. ~~Their loadings in the global atmosphere have increased substantially.~~ Scientists have suggested that~~ the~~ scattering aerosols could greatly offset the warming effects of greenhouse gases (Kiehl and Briegleb, 1993) while~~ the~~ absorbing aerosols~~components~~ might further exacerbate~~ the~~ global warming (Jacobson 2002). The global mean direct radiative forcing~~s~~ (DRF~~s~~) of scattering aerosols, fossil fuel black carbon (BC)~~BC~~ and~~ the~~ all~~total~~ aerosols ~~wereas~~ was estimated to be approximately~~about~~ -0.55, +0.2~~,~~ and -1.04 W/m^2, respectively (Forster et al., 2007; Reddy et al., 2005), at the top of atmosphere (TOA), thus changing ~~the~~ atmospheric circulations and the hydrological cycle in different ways (~~.~~Menon et al., ~~(~~2002; Wang et al., 2015)~~ suggested that the changes in the trends of rainfall in China over the past 5 decades might be related to the variations of in BC in Asia regions. Wang et al. (2015) indicateds that the East Asian summer monsoon circulation could become weaker due to the cooling effects of the aerosols but could become stronger due to the warming effects of BC~~.

~~Although m~~Many studies of~~n the~~ aerosol radiative forcing and its climate effects have been carried out over the past two decades at~~in~~ both global and regional scales ~~and using based on~~based on model simulations and observations~~ in the past two decades~~ (e.g., Penner et al., 2001; Bellouin et al., 2003; Liao and Seinfeld, 2005; Wu et al., 2012; Wang et al., 2015~~; etc.~~;~~,~~ etc.)~~;,~~ however, large uncertainties remain~~still exist~~. Forster et al. (2007) ~~pointed out~~noted that the global mean DRF varied from +0.04 to

-0.63 W/m^2 for ~~the~~ total aerosols and from +0.1 to +0.3 W/m^2 for BC. The ranges were larger at~~in~~ regional scales, especially in high aerosol emission~~tted~~ regions (Zhuang et al., 2013a). The DRF uncertainties ~~would~~ subsequently result in large biases of the aerosol-related climate effects. There are many factors that affect~~ing~~ the simulated radiative forcing, including the aerosol optical properties, which are related to ~~the~~ aerosol emissions, size distributions, profiles, compositions, and mixing states (Holler et al., 2003; Ma et al., 2017), as well as the~~,~~ surface albedo and clouds (Ma and Yu, 2012; Forster et al., 2007). The related uncertainties could be substantially reduced ~~substantially~~ if the observed aerosol optical properties were determined ~~figured out~~ and used (Forster et al., 2007).

With the rapid increase in population and ~~growth in~~ economic~~s~~ growth, ~~the~~ air pollutant emissions are much higher in East Asia than in ~~the~~ other regions (Zhang et al., 2009). Additionally, dust aerosols from desert regions are always transported to northern and eastern China or even further afield (Wang et al., 2009; Sun et al., 2012; Li et al., 2015a). Consequently, aerosols in China ~~become~~ frequently experience large ~~in~~ loadings and complicated ~~in~~ compositions and spatial distributions (Zhang et al., 2012), especially in urban agglomerations or megacities (~~e.g.:~~e.g.,~~:~~ the Yangtze River Delta,~~:~~ YRD). Therefore, ~~it is necessary to clarify~~ the aerosol optical properties in the YRD must be clarified via~~through~~ observations, which is a premise for accurately estimating the ~~aerosol~~ radiative effects of aerosols ~~and also~~ and for ~~in favor of~~ improving ~~the~~ aerosol model performance~~s~~ ~~on aerosols in~~over the eastern region of China. Recently, numerous~~substantial~~ observation~~al~~-based studies have been conducted on both ~~the~~ surface (e.g., Bergin et al., 2001; Xu et al., 2002; Zhang et al., 2004; Xia et al., 2007; Yan et al., 2008; He et al., 2009; Fan et al., 2010; Cai et al., 2011; Xu et al., 2012; Wu et al., 2012; Zhang et al., 2015; Yu et al., 2016; Deng et al., 2016~~; etc.~~; Zhuang et al., 2017;~~;~~ etc.) and columnar (e.g., Chiang et al., 2007; Pan et al., 2010; Yu et al., 2011; Zhao et al., 2013; Tao et al., 2014; Zhu et al., 2014;

Che et al., 2011; 2013; 2014; 2015a, b, c; Xia et al., 2016; Zheng et al., 2016; Qi et al., 2016, etc.) aerosol optical properties (and DRFs), especially ~~those~~ in China. However, surface data can~~ould~~ not completely represent the total ~~whole~~ conditions of ~~the~~ aerosols in the atmosphere as these aerosols~~and they~~ are highly affected by the variations ~~of~~ in boundary layers. The related~~Its~~ deficiency could be solved ~~usingmade~~with ~~up by the~~ measurements of the columnar aerosols. For ~~the~~ studies of surface aerosols, people mainly focus on the aerosol ~~their~~ absorption coefficient (AAC) and scattering coefficient~~s~~ (~~AAC and~~ SC). ~~Previous iInvestigations stated that both AACs and SCs in urban areas are frequently stronger than those at other sites, reaching. They were ~30 and 338 Mm^{-1} in the western YRD (Zhuang et al., 2017).~~ For columnar aerosol observations, the detailed aerosol optical and physical properties can~~ould~~ be obtained, including the aerosol optical depth (AOD), refractive index, Ångström exponent~~s~~ (AE), ~~and so on,~~ etc. Che et al. (2015a) introduced a systematic long-term measurement of the countrywide total ~~aerosol~~ AOD and AE in China from 2002 to 2013~~,~~ and indicated that the annual mean AOD~~s~~ were 0.14, 0.74 and 0.54 for~~at the~~ rural sites, urban sites, and ~~in~~ eastern China, respectively. There are also some researches focusing on the aerosol optical properties i~~I~~n the YRD~~,~~ (Pan et al., ~~(~~2010; ~~) showeds that the AOD at 440 nm and the AE in coastal areas (eastern YRD) whereas about 0approximately 0.74 and 1.27, respectively.~~ Yu et al., ~~(~~2011; ~~) and~~ Zhuang et al., 2014a; Qi et al., ~~(~~2016) ~~indicated that the total aerosol AOD exceeded 0.6, and that its single scattering albedo (SSA) was ~0.88 over thein lake and urban areas of the central to east to eastern YRD. Zhuang et al. (2014a) indicateds that a one-year observation of theed AOD and AE of the total aerosols in the urban area of Nanjing (urNJ, western YRD) was similar to the results of Pan et al. (2010), but that differences existed~~. In addition to the aerosol optical properties, the observation~~ed based a~~-based aerosol DRFs ~~are~~ have also been estimated around the world (such as those found in~~:~~ Markowicz et al., 2008; Khatri et

al., 2009; Kuhlmann and Quaas, 2010; Alam et al., 2011, Zhuang et al., 2014a, and Xia et al., 2016). However, almost allall of theseir investigations focused on the total aerosol forcings. For example, Xia et al. (2016) stated that the regional mean aerosol DRF in China was approximatelybout -16~-37 W/m^2 at the TOA and approximatelyabout -66~-111 W/m^2 at the surface when the solar zenith angle was approximatelybout 60°.60°.

Although considerable studies ofn the observed columnar aerosol optical properties have been carried out in China andor even within the YRD (one of the regions with the fastest rapidest urbanization regions in China), gthere still have gaps in thcneed to be improved for the current observations remain, especially in the urban areas of thosee regions with intensivee human activities. In the YRD or eastern China, most of the investigations ofn the aerosol optical properties were have focused on the coastal, lake and rural regions (Pan et al., 2010; Yu et al., 2011; Che et al., 2015a; Qi et al., 2016) of the central to east to eastern YRD. And . Additionally, most of these studiesm only address only the total aerosol optical properties (independent of modes and compositions), except for the work of Qi et al., (2016)., whichwho They also introduced theso made an introduction on the aerosol physical parameters and size fractional SSA of anin eastern coastal city (Hangzhou, hereinafter written asshort for urHZ) of the YRD, which is. There is about 3approximately 300 km of urHZ away from the western YRD. As implied in Zhang et al. (2012), aerosols are have complicated in compositions and spatial distributions, especially in fast rapidly developing regions (such as YRD). Thus, considerablelarge differences might exist of in the aerosol optical and physical properties might exist to degrees among the sites within the YRD. Additionally, none of researchesstudiesresearch mentioned above have studied the aerosol DRFs. Some investigations ofn the columnar aerosols in the western YRD (urNJ) werehave been carried out in by Zhuang et al. (2014a), but significant issues (not

considered in their works) still require further study need to be further addressed, such as the size fractional optical parameters and the DRFs of different aerosol components, as well as the aerosol physical size fractional aerosol physical properties of the different size fractions. Therefore, it's still necessary to make a more integrated investigation of the aerosol optical and physical properties, as well as their DRFs in the YRD, is still required. In this study, the unaddressed issues for the western and whole YRD region mentioned above will be studied all included based on the measurements of a Cimel sun -photometer in urNJ, combined with a radiation transfer model (TUV, Madronich, 1993). Additionally, the aerosol types and mixings in the region will be further identified and discussed based on the relationships among the aerosol optical properties. Third, the observed aerosol profiles, which have not previously been considered before in the YRD, are discussed and further used and discussed here to calculate the aerosol DRFs. The results of this study will would be advantageous to further understanding the characteristics of aerosols over the eastern regions of China. Additionally, this work will help to improve aerosol model performances as well as the modelled on the aerosol and its climatice effects in the relevant regions. Firstly Because, first of all, the observed aerosol parameters can be used for data assimilation to obtain more accurate inputs (including improved initial conditions and air pollutant emissions) for the model (Jiang et al., 2013 and Peng et al., 2017). Second, a more precise aerosol refractive indexes and size distributions used in these numerical models will yield a more reasonable aerosol loadings and DRFs (Ma et al., 2017). Third, both the aerosol optical properties and DRFs can be used to validate the simulations.

The methods are described in Section 2. The results and discussions are presented in Section 3, followed by the conclusions in Section 4.

2 Methodologies

2.1 Sampling station and instruments

The observation site (Urban Environmental Monitoring Station of Nanjing University) is located in the downtown area of Nanjing City (hereinafter shortened to urNJ; located at 32.05°–05° N, 118.78°–78° E), in the western YRD. The site is on the roof of a 79.3-m-tall building, surrounded by few higher obstacles and with no industrial pollution sources within a 30 km radius. However, there are several main roads with apparent traffic pollutions. Detailed information about the site is available from Zhu et al. (2012).

The columnar aerosol optical properties and physical characteristics of the site were measured by the Cimel sun photometer (CE-318, Holben et al., 1998) during the period from Apr 2011 to Feb 2014. Routine maintenances and calibrations was performed during the observational period. Due to the malfunctions of the instrument and the problems with data transmission, the data from May to Sep 2012 and from Aug to Dec 2013 are invalid and were thus excluded. The wavelength-dependent optical depth (AOD) and Ångström exponents (AE) of the total aerosols were directly measured by CE-318, while the following variables, including the aerosol size distributions, fractionated (fine and coarse) aerosol effective radius (R_{eff}), mean radius (R_{mn}), volume concentrations (Vol), wavelength-dependent size fractional optical depths of the various sizes of scattering, absorbing and total aerosols, aerosol SSA single scattering albedo (SSA); and the, as well as wavelength-dependent refractive indices, are derived from the DOBVIC algorithm Version 2 (Dubovik et al., 2000; 2006). This algorithm has been widely used by the Aerosol Robotic Network (AERONET) and the China Aerosol Remote Sensing Network (CARSNET), while and the products have been used globally, as introduced in the Introduction, due to their high accuracies. The errors for the AOD,

absorption AOD (AAOD) and ~~,~~ SSA are~~is~~ 0.01, 0.01 and 0.03, respectively (Yu et al., 2011; Li et al., 2015c). The errors of the fine and coarse aerosol SSAs are~~is~~ 0.037 and 0.085, respectively (Xu, 2015). The errors of the refractive index are~~is~~ 0.04 for the real part and 0.0025-0.0042 for the imaginary part (Yu et al., 2011)~~. And~~ . Additionally, the error of the volume size distribution is less than 10% in the peak regions but is ~~while about 3~~approximately 35% in valley ~~region~~ or interval regions for the~~between~~ fine and coarse modes (Yu et al., 2011). Detailed descriptions of~~on~~ CE-318 and the corresponding observations from~~in~~ CARSNET are available ~~in~~ from Li et al. (2015a) and Che et al. (2015a). For comparison, the 550 nm AODs and SSAs are calculated based on the given AODs at other wavelengths and AEs (Angstrom. 1929):

$$AOD_{550nm} = AOD_{440nm} \times (\frac{550_{nm}}{440_{nm}})^{-AE_{440/870nm}} \quad (1)$$

$$AAOD_{550nm} = AAOD_{440nm} \times (\frac{550_{nm}}{440_{nm}})^{-AAE_{440/870nm}} \quad (2)$$

$$SSA_{550nm} = \frac{AOD_{550nm} - AAOD_{550nm}}{AOD_{550nm}} \quad (3)$$

For~~To make~~ a further comparison, ~~the~~ concurrent observations of the surface total ~~aerosol absorption coefficient (~~AAC~~)~~ and ~~Ångström exponents (A~~AE~~)~~ measured by a 7-channel Aethalometer (model AE-31, Magee Scientific, USA, Hansen et al., 1984; Weingartner et al., 2003 and Arnott et al., 2005) are used. The d~~D~~etailed calculations and corrections of the AAC at the site ~~can~~ould be found in were presented by Zhuang et al. (2015). Additionally~~In addition~~, the monthly mean ~~optical depth (~~AOD~~)~~ and ~~Ångström exponent (~~AE~~)~~ of the total aerosols from the satellite-based ~~of~~ Moderate Resolution Imaging Spectroradiometer (MODIS) were used ~~to assist~~in the analysis.

Based on the observed wavelength-dependent aerosol optical properties, the ~~aerosol~~ DRF~~direct~~

radiative forcing (DRF) of the aerosols in urNJ is investigated using thea radiation transfer model TUV (Madronich, 1993). Only clear-—sky DRFs are addressed here because almost allall of the measurements are carried out in free sky conditions. The solar component of the radiative transfer scheme in the TUV model follows the δ-Eddington approximation. In addition to the aerosol optical properties, the surface alebdoalbedo (Palancar and Toselli, 2004) and the aerosol vertical profiles (Forster et al., 2007) might also have significant influences on the DRF. Thus, the wavelength-dependent surface albedo from MODIS, the annual and seasonal mean aerosol profiles from the Cloud-Aerosol Lidar and Infrared Pathfinder Satellite Observations (CALIPSO) and the Polarization-Raman Lidar (PRL) in Nanjing arewould be included when assessing the aerosol DRF. The aerosol DRF in this study is defined as the difference in the net shortwave radiative fluxes whenbetween including orand excluding the aerosol effects at the TOA and surface. The gGas absorptions in the atmosphere were set to be constant. The scattering aerosol'ss SSA was set to 0.9999 (similar to that of sulfatesulphate sulfate or nitrate, Li et al., 2015b) when calculating its DRF. The DRF of the absorbing aerosols is derived from the differences between the total and the scattering aerosol DRFs.

3 Results and discussions

3.1 Optical properties of the aerosols

Unless otherwise specifiedIn this section, the 550 nm optical depthAODs, SSAssingle scattering albedo and 440 nm refractive indices of the aerosols hereinafter all representare the ones discussed as representationsves offor the temporal variations and frequency distributions of these three kinds of the aerosol optical parametersat 550, 550 and 440 nm, respectively. In addition to the totalwhole mode

aerosols, the size-dependent ~~fractional~~ (i.e., the fine and coarse fractions~~ones~~) aerosol optical properties of the different types~~components~~ (scattering and absorbing aerosols) are also discussed in this section. Therefore, there are ~~altogether~~ nine types of aerosols~~:~~, ~~including the~~ total aerosols (TA), total fine aerosols (FA), total coarse aerosols (CA), scattering aerosols (SA), fine scattering aerosols (FSA), coarse scattering aerosols (CSA), absorbing aerosols (AA), fine absorbing aerosols (FAA), and coarse absorbing aerosols (CAA).

Table 1 summarizes~~y~~ the statistics of the aerosol optical properties during the study period in urNJ. The mean total aerosol ~~550 nm optical depth (~~AOD~~)~~ ~~of the total aerosols~~ is 0.65, and the SA's~~scattering aerosols~~ account for as much as~~large as~~ ~~about 9~~approximately 93.84% of this category. Fine mode ~~aerosol~~ AOD~~s~~ (FAOD), fine mode scattering AOD (FSAOD) and fine mode absorbing AOD (FAAOD) account~~s~~ for 81.53%, 81.97% and 56.09% of the total AODs, scattering AODs (SAODs) and absorbing AODs (AAODs)~~ at in this wavelength~~, respectively, implying that coarse aerosols~~ is more~~ absorb more~~ing~~ than~~ the~~ fine ones. The 440/870 nm AE of the total, scattering and absorbing aerosols are ~~about 1~~approximately 1.20, 1.19, and 1.32, respectively. Fine aerosols have much higher~~larger~~ AEs, which can be~~,~~ 0.4-0.5 greater~~larger~~ than those of the total aerosols. Overall, the absorbing aerosols have smaller sizes than the scattering ones in all modes, ~~but~~ especially in the coarse mode, which is consistent with the results from~~of~~ the surface aerosols at the site (Zhuang et al., 2017). ~~The aAnnual mean 470/660 AAE (from AE 31) and 450/635 nm SAE (from Nephelometer Model Aurora 3000) of the near surface aerosols are 1.58 and 1.32, respectively, at the site during the period from March 2014 to Feb 2016 (Zhuang et al., 2017).~~ The mean ~~550 nm~~ SSA~~s~~ of TA, FA and CA is~~are~~ 0.93, 0.95 and 0.82 ~~for the total, fine and coarse aerosols~~, respectively, further implying that the coarse aerosols have different compositions ~~and have considerably greater~~much stronger abilities~~y~~ to absorb solar

shortwave wave radiation thanthan the fine aerosols. The cComparisons also indicate that surface aerosolsl (SSA=0.9 in Zhuang et al., 2017) areis a little more slightly more absorabsorptiveption than the columnar aerosols in urNJ. The aAnnual mean surface SSA at 550 nm for the total aerosols is little slightly smaller (0.9) than the column one. The mean 440 nm refractive index is about 1approximately 1.44+0.0084i. The table also implies that the western YRD could suffer very serious particle pollutions.

Table 1

3.1.1 Seasonal variations of in the aerosol optical properties

Figure 1 presents the monthly variations of in the 550 nm AOD (a), SAOD (b) and AAOD (c) as well as the contributions of their fine and or coarse modes to their corresponding totals. The tTemporal variations of in the total aerosol AOD areis consistent with those of SAOD due to the significantly large ratio of SAOD/AOD. The AODs are all considerably high in the winter due to thea more intense emissions of the trace gases and particles (Zhang et al., 2009). Additionally, they are also high in spring and summer under the influences of dust, high efficiencies of moisture absorption growth and chemical transformationHowever, thea long distance transport ofed dust aerosols from northern China in the spring as well asnd the high efficiencies of moisture absorption and scattering aerosol chemical transformations in the summer (Li et al., 2015a) also lead to higher AODs in these two seasons. Therefore, the dust episodes, relative humidity (RH) and chemical processes weaken the seasonal variations of the total AODs are not so obviouspurely by inducinged by the emissions in urNJ, in the western YRD. TInstead, these processes influences are prominent in the AOD seasonality for theof different aerosol types within thein different size segments. The largest AODs appear in the spring for the coarse scattering and absorbing aerosols, but the largest AODswhereas they appear while in the

summer for the fine aerosols~~ones~~ in urNJ. The figure also implies that the scattering aerosols might have different size distributions than~~from~~ the absorbing aerosols. The fine mode fraction ~~rate~~ is 0.83 (peaking at 0.97) for scattering aerosols and is~~while~~ 0.56 (peaking at 0.83) for absorbing aerosols. ~~In other words, the fine aerosols have different compositions than from the coarse ones.~~ It's noting that AOD in August does not include the ones in 2012 and 2013. Coincidentally, air pollution has been controlled since 2012 in Nanjing due to hosting international events in Aug 2013 and 2014. August AOD in 2011 is 1.18, much higher than those in 2012 (0.75) and 2013 (0.63) as referred from the MODIS retrievals. As a result, the AOD in August shown in Figure 1 is "unusually" high.

Figure 1

The aerosol ~~Ångström exponents~~AEs also have substantial~~ly~~ seasonal variations, especially for the absorbing aerosols, as illustrated in Figure 2. The seasonal variation of the fine aerosol AE is highly consistent with the coarse one for the absorbing aerosols while it is opposite for the scattering aerosols.~~For both the each component (scattering and or absorbing one aerosols), the seasonal variations of in the its fine and coarse AEs are well agree well with each other, which are closeall being close to zero line in the summer.~~ Nevertheless, all AEs in the summer are the closest to 0 possibly due to the effects of high RH~~relative humidity~~ (Zhuang et al., 2014a). The whole mode AE of each aerosol type is determined by the both variations ~~of~~ in the AEs in each mode and the fine mode fraction. Therefore, the smallest AEs appear~~s~~ in the summer (0.74 in July) for the total absorbing aerosols but appear ~~while~~ in the spring (0.94 in Mar) for the total scattering aerosols. Similarly, the total aerosol AE is determined by ~~the~~ both the variations of each aerosol type's AE and the ratio~~fraction rate~~ of the scattering (or

absorbing) aerosols to the totals. AndSimilar to the AOD, the seasonalityy of the total aerosol AEs is more consistent with that of the scattering aerosols. The figure also indicates that the scattering aerosols have much larger sizes than the absorbing aerosols, especially those in the coarse mode. Further comparisons indicates that the seasonal variations of the columnar SAE and AAE are consistent with their surface ones of the surface SAE and AAE (results not shown hereZhuang et al., 2017) values at the site.

Figure 2

In addition to AOD and AE, the monthly variations of in the aerosol SSAssingle scattering albedo (SSA) and refractive indices are also investigated, as shown in Figure 3. SSA is affected by both scattering and absorbing aerosols, as well as their relative contributions. The fine particles have much strongerare much more scatterings than the coarse aerosols. However, the coarse aerosol SSAs hasves more significant seasonalityTheir SSAs have relatively weaker seasonality. Overall, both FSSA and CSSA are relatively smallerer in summer as compared than into those ofthan in the otherthe warmer seasons, although they wereare considerable considerably large in August 2011, implying that the two types of aerosols in the summer are more absorbing in summer than those in the other seasons. The total aerosol SSA is somewhere in between the FSSA and CSSA and dependsing on the ratios of the FAOD to AOD. Thus, these an SSAs haved it has different seasonal variations from the FSSA or CSSA. SSA is also rather the smallest in spring due to the largest contribution of coarse aerosols occurring in this season. The aerosol refractive indices also show considerablesubstantial seasonality. The real part is large in the spring but small in the summer, which is similar to what was observed in Taihu Lake in

the central YRD (Yu et al. 2011). The imaginary parts show relatively weaker seasonal variations than those of the real parts.

Figure 3

To provide a more quantitative knowledge, Table 2 summarizes the abovementioned seasonal means with the corresponding standard deviations for the all the aerosol optical properties. It providinges more quantitative variations of in the aerosol optical properties than incompared with the figures above. And it's more obviously reflecting the different variations of the optical properties among different aerosol categoriesThe sSeasonal mean 550 nm AOD, SAOD and AAOD vary from 0.59 in the fall to 0.75 in the summer, from 0.55 in the fall to 0.70 in the summer, and from 0.037 in the fall to 0.050 in the spring, respectively. For example, CAOD, CSAOD, CAAOD account for the majority of the AOD, SAOD and AAOD in the spring, with the ratios of 30.1%, 27.9%, and 58.1%, respectively. FAOD, FSAOD, FAAOD account for the majority of the AOD, SAOD and AAOD in the summer, with the ratios of 90.5%, 91.2% and 70.2%, respectively. As discussed above, the seasonal variations of the total mode aerosol AEs and SSAs are different from the ones in each mode. The seasonal mean 440/870 nm SAE and AAE values vary from 0.98 in the spring to 1.38 in the fall, and from 0.78 in the summer to 1.50 in the winter. The sSeasonal mean FSSA and CSSA values vary from 0.940 in the summer to 0.956 in the winter and from 0.787 in the summer to 0.834 in the spring, respectively. The real part of the aerosol refractive index has a relatively stronger seasonality than the imaginary part. Their greatestlargest values are all found in spring. Comparisons indicate that the seasonal variations of the optical properties areis highly spatially inhomogeneous spatially within the

YRD. As indicated byin Che et al. (2015a) and Qi et al. (2016), the largest AOD was found in the spring, while the lowest one appeared in the summer in urHZ, another city on thein eastern coast of the YRD. In Taihu Lake, a rural site in the central YRD, the lowest AOD appeared in the winter (Pan et al., 2010; Yu et al., 2011). Additionally, the aerosols absorb the mostare the most absorbing in the winter in the central regions of the YRD (Taihu Lake and urHZ), and their SSAs are as small as 0.88 (Yu et al., 2011 and Qi et al., 2016). The aAerosols in the western YRD (urNJ) are more scattering than those of the preceding areas,theirs and the smallest SSA values appears in the spring during the sampling periods. Nevertheless, AE variations are more consistentcy with each other betweenamong these sites, being , being smallest in the spring and largest in the fall.

Table 2

3.1.2 Frequencies of the aerosol optical properties

All AODs and SSAs follow a near lognormal pattern, and almost allall of the AEs and refractive indices follow a unimodal pattern (Figure 4). The ranges around their means are dominantted, accounting for at least 60% ofto their total data samples during the entire study period. Similar to the temporal variations, the frequency distributions of the total aerosols (not shown) are also highly similar to thosee ones of the scattering aerosols in both the fine and coarse modes.

The frequencies of the absorbing aerosol AEs differ from thoseare different of from the scattering aerosol AEsones, which are written as so isand the frequencies of the AE of absorbing aerosols in fine mode (FAAE) and also differs from the AE of absorbing aerosols in coarse mode (CAAE). The occurrences of smaller CAAE (or large FAAE, AAE) values are also relatively high. However, the large FAAE values, i.e., those exceeding 2.5, also contributehas contributions (more than 5.4%). Both

~~the fine and coarse absorbing aerosols have much smaller sizes than the scattering aerosols of~~at ~~the same modes.~~ Due to different absorbed fractions among coarse, fine and total aerosols, the curve of CSSA (FSSA) has a leftward (rightward) shifting compared with that of SSA, peaking around 0.84 (0.97).~~The f~~~~Frequency distributions of SSAs also implyies that the coarse aerosols are more absorb moreing than the fine aerosols. Consequently, the frequencies of SSAs peak between 0.95 and 0.97, and between 0.80 and 0.84 for the fine and coarse mode aerosols, respectively, in urNJ during the study period.~~ The f~~F~~ine aerosol SSAs were concentrated in a~~s~~ more ~~in a~~ narrow range (~0.1~~from 0.89 to 0.99~~) than the CSSAs were (~0.3~~from 0.64 to 0.96~~). For the refractive index, the frequencies peak around~~between 1.39 and~~ 1.42~~,~~ and ~~between 0.007 and~~ 0.00~~89~~ for the real and imaginary parts, respectively, in urNJ during the study period.

The frequency patterns of the aerosol optical properties also have substantial seasonality (not shown here). Overall, the curves ~~would~~ shift left-ward in low value seasons and right-ward in high value seasons. In the summer, the AOD curves might even have two peaks for the scattering or total aerosols, which are similar to the observations in Taihu Lake (Yu et al., 2011). ~~For SAE, the peak shifts left ward by 0.2 in the spring by 0.2 and, but right ward by 0.2 in the fall by 0.2. For SSA, both the fine and coarse aerosol SSA frequencies showhave a left ward shifts from the annual mean in the summer compared to the annual one, which is the opposite trend to that ofas thee frequency of the total SSA because the fine aerosol AODs dominate the signal, accounting for about 9approximately 91% of the totals. The real part of the frequency in the spring showshas a significant right ward shift compared to the average overat in the entire study period, peaking between 1.46 and 1.50 (not shown). The frequency of the imaginary part frequency in the winter showshas a significant leftward ward shift compared to that ofin the study period, peaking between 0.001 and 0.003 (not shown).~~

3.1.3 Comparisons with MODIS AOD, AE and surface aerosols

The AOD and AE observed by CE-318, to degrees, are well correlative ~~in reasonable agreement~~ with those from MODIS in terms of their seasonal variations and magnitudes (Figure 5). The linear correlation coefficients are 0.~~75~~71 and 0.~~86~~67 between the monthly mean CE-318 ~~AOD~~ and MODIS AODs and between the monthly mean CE-318 ~~AE~~ and MODIS AEs, respectively. The AOD ~~at 550 nm~~ from MODIS is greater (~1.2 times) ~~larger~~ than that from CE-318, with an average value of 0.~~82~~80 during the study period. The slop of the linear fitting is 1.12 for AOD in urNJ, similarly to that in central China (slope=1.16, Dong et al., 2013). The mean AE at 412/470 nm from MODIS is ~~about~~ ~~1~~approximately 1.~~43~~42. The standard deviations of the AOD and AE values are much larger for ~~rom~~ CE-318 than for ~~rom~~ MODIS, possibly due to the ~~a~~ higher temporal resolution of the CE-318 observations.

Figure 5

The columnar AAOD and AAE values from CE-318 are ~~fairly~~ less related to the surface aerosol absorption coefficient (AAC) and AAE from AE-31 (Figure 6). ~~However, the relationship between~~ the ~~AAOD and AAC, or that between the column and surface AAEs, is worse than that between the values of CE-318's and MODIS' values. Although~~ Because surface aerosols ~~could be affected by their transport, they are~~ ~~it is~~ mainly affected by ~~from~~ local and regional emissions, and their ~~its~~ loadings are highly related to the degrees of ~~the~~ boundary layer development (~~. As suggested by~~ Zhuang et al., ~~(~~2014b and 2015)~~, surface aerosol loadings are considerably low in the afternoon and during the~~

summer, times when the boundary layers are well developed. The columnar AAODs could alsoadditionally be further affected by the emissions and transportations in the upper atmosphere and it is are less affected by the boundary height thancompared with the surface AAC is, thus contributing to a relatively worse relationship between the AAOD and AAC. The surface AAE is more concentrated in a narrower range and it is larger (1.6) than that from CE-318, implying that the surface absorbing aerosols are finer and fresher. The linear correlation coefficients are 0.39 and 0.41 between the AAOD and AAC and between the columnar and surface AAEs are 0.39 and 0.41, respectively, which areis slightly worse than those between FAAOD and AAC (0.46) and between the columnar FAAE and surface AAE (0.47).

Figure 6

3.1.4 Briefly discussions

Ground based observed aerosol observationss have much higher temporal resolutions thancompared with satellite retrievals. The observed columnar optical properties could mitigate make up the deficienciesy of surface aerosol data on one hand, and make us better understandResults here allowing us to for a better understanding of the characteristics of the aerosols in the YRD on the other hand. AndAdditionally, theyse propertiesy might be also useful for improving aerosolthe model performances on the aerosols and their radiative effects in the YRD or eastern China as referred in Introduction. The observed aerosol parameters could be used for data assimilation, which can produce more accurate initial conditions forof the model and more accurate variations of the aerosol emissions (Jiang et al., 2013 and Peng et al., 2017). The data set of the optical properties ofin most cof the climate

~~or air quality models are frequently from a given refractive index and is~~which is ~~homogeneous in time and space. Therefore, the use of a more precise aerosol refractive index used in numerical models would yield a more reasonable aerosol optical properties and radiative forcings in the observed regions and their surroundingsaround. Furthermore, the observed aerosol optical properties could be also be used to validate the simulations~~.

~~As mentioned in the Introduction, m~~Most studies o~~f~~n the aerosol optical properties in China mainly focus on the AOD and AE of the short-term total aerosols ~~in short term~~ (i.e., episodes, Che et al., 2013; Zheng et al., 2016; Che et al., 2015b), although~~. Studies on~~ the annual (Yu et al., 2011) and decadal (Che et al., 2015a) scale aerosols have been also carried out in recent years ~~using~~based ~~on~~ based on CE-318 measurements. ~~Che et al. (2015a) indicated that the long ternlong term averages of the total aerosol AOD at 440 nm and AE at 440/870 nm in urban areas were about 0~~approximately 0.75 ~~and 1.05 in northern China, 0.98 and 1.09 in Sichuan Basin, 0.78 and 1.36 in the Pearl River Delta region (PRD), 0.65 and 1.0 in northeastern China, 0.66 and 89 in northwestern China, 0.92 and 1.0 in central China, and 0.9 and 1.25 in the coastal areas of the YRD, respectively.~~ Results here show that t~~T~~he mean AOD ~~at 440 nm~~ in urNJ is greater~~larger (0.84)~~ than those~~at~~ in northern China and the PRD but is smaller than those of the~~at in~~ coastal cities of the YRD. The AE is larger in urNJ than ~~a~~Aerosols in northern and central China ~~have larger sizes (smaller AE) than those in the western YRD~~. Che et al. (2015a) further suggested that those~~e~~ aerosols in urban areas likely had larger AODs and AEs than those in mountain and desert areas. It's~~, so did~~ the same in urNJ. Qi et al. (2016) showed~~presents~~ that the aerosol SSAs~~single scattering albedo~~ at 440 nm in urHZ are~~is~~ ~~about 0~~approximately 0.90, 0.92 and 0.70 for the total, fine and coarse aerosols, respectively, also implying that the coarse aerosols ~~are more~~ absorb more~~ing~~ than the fine ones. Our measurements show similar results ~~to theirs~~. However, the

aerosols in urNJ scatter more~~are more scattering~~ than those in urHZ in both the fine and coarse modes, also revealing the inhomogeneous distributions of the aerosol compositions in the YRD. ~~Although some studies ofn the columnar aerosol optical properties based observations have been carried out in the YRD using observational data (Pan et al., 2010; Yu et al., 2011; Zhuang et al., 2014a; Che et al., 2015a, Qi et al., 2016), T~~this study ~~here~~ further augments ~~fill the gaps of~~ the current observations of the aerosol optical properties in the YRD compared with previous studies. ~~Based onon the authors'~~ ~~previous research (Zhuang et al., 2014a), a more comprehensive and systematic analysis ofn the fractionated optical properties of different aerosols types are~~ is ~~also~~additionally carried out here. ~~The results would~~ allow a ~~be advantageous to further understanding of the aerosols over eastern China.~~

3.2 Physical properties of the aerosols

In addition to the optical properties, the aerosol physical properties, including the volume size distributions, mode--dependent sizes (radius) and volume concentrations, were~~are~~ also retrieved. Figure 7 shows the volume size distributions of the aerosols in different seasons (Figure 7a) and at~~in~~ different AOD (or polluted) levels (Figure 7b) in urNJ. ~~The figure~~It shows that the aerosols in urNJ have a typical bimodal structure in their volume size distributions in all seasons, presenting ~~a~~ two-mode lognormal distributions in both the~~:~~ fine (radius < 0.6 μm) and coarse modes (radius > 0.6 μm). Their annual peaks appear at ~~the~~ radi~~us~~ of 0.148 μm for the~~in~~ fine mode and 2.94 μm for the~~in~~ coarse mode. ~~Similar to the aerosol optical properties, t~~The aerosol volume size distributions also have~~s~~ substantial seasonality. Dust episodes lead to the ~~the~~ peak values in the spring being much smaller in the fine mode than those in the coarse mode, which is the opposite trend than ~~those for to that in~~in the other seasons (especially in the summer). Therefore, the mean radius of the aerosols increases significantly in the

spring due to the ~~a~~ high proportion of coarse particles, leading to a smaller AE, as discussed in the previous sections. In the summer, the curve has a right-ward shift, showing a larger aerosol size in both the fine and coarse modes due ~~to~~to the high hygroscopic growth efficiency. The fine particles are dominant~~te~~ in the summer and result in large AE values, opposite to the patterns ~~what is~~ in the spring. The aerosol volume size distribution varies with different AOD values (Figure 7b) in urNJ. Overall, the peak value has a substantial right-ward shift with increasing AOD for fine aerosols while a slightly leftward ~~ward~~ shift for coarse aerosols, implying that the growth of the fine aerosols is advantageous to enhance the aerosol radiative effect. In urNJ, both fine and coarse particles ~~basically~~ have approximately the same levels when AOD is below ~0.8~~. And~~. In addition, the fine aerosols begin to dominate more when AOD ~~exceeds~~ >0.8. The results here are ~~rather~~ mostly consistent with the ones ~~in~~ from Yu et al. (2011), Qi et al. (2016), and Zheng et al. (2016). However, the figure here further ~~reflects~~ indicates that both fine and coarse particles themselves ~~could~~ might cause very serious haze pollutions in YRD, ~~leading to~~ showing considerably high peak~~ing~~ values in both fine and coarse modes, which ~~being found. This~~ has not been observed in previous publications. The aerosol size distributions here are also very useful for optimizing numerical models. ~~A more precise aerosol size distribution would make the models more accurate in describing the aerosol transportation and, deposition as well as its radiative effects (Ma et al., 2017) in YRD or eastern China.~~

Figure 7

To further investigate the physical features, the seasonal variations ~~of~~ in the aerosol effective and mean radius~~, as well as~~ and the volume concentrations in urNJ are ~~further~~ presented in Figure 8. The

mean effective radius, which is generally smaller than the mean one in all modes, is ~~about~~ ~~0~~approximately 0.34, 0.16, and 2.18 μm for the total, fine and coarse aerosols, respectively, during the study period. ~~It~~ This figure ~~additionally~~ also ~~reflects~~ shows ~~that the aerosols in urNJ are dominated by the fine particles, as discussed previously.~~ The seasonal variations ~~of~~ in the radi~~i~~uses have a strong~~good~~ anti-correlation to ~~the one~~ that of the AEs (Figure 2). Both the fine and coarse aerosol radi~~i~~us are larger in the summer than in the other seasons ~~due to the moisture absorption growth of the aerosols. However,~~ while the total aerosol radius is much larger in the spring ~~due to thea larger coarse fraction~~. ~~Differingrent~~Unlike ~~from~~ the radius, the seasonal variations ~~of~~ in the volume concentrations of the~~between~~ fine and coarse aerosols are different, peaking in the spring for coarse aerosols~~,~~ and ~~peaking~~while in the summer for fine aerosols. Although both the fine and coarse aerosols have th~~e~~e same annual volume levels in urNJ ~~annually~~, their contributions to the total aerosol volumes vary significantly with season~~s~~. The coarse aerosols ~~directly~~ lead~~s~~ directly to the largest total aerosol volume peaking in the spring ~~for the total aerosols~~.

Figure 8

3.3 Aerosol classification based on ~~its~~ optical properties

The aerosol clusters, to a certain degree, can~~ould~~ be identified based on the relationships between SSAs at 491 nm and AEs at 491/870 nm~~,~~;~~,~~ between the real refractive index (RRI) at 670 nm and the AE at 491/870 nm~~,~~;~~,~~ ~~as well as~~and between the SSA differences (dSSA=SSA_{870nm}-SSA_{491nm}) and AE at 491/870 nm, as presented ~~in Rn~~ by Russell et al. (2014)~~,~~ ~~whichho~~ They proposed a Mahalanobis Classification based on "a priori" information for each type of aerosol source (~~e.g.~~e.g.~~,~~ dust, urban,

biomass aerosols). Different aerosols ~~then~~ would then be mostly concentrated within the corresponding ellipses of a two-dimensional scatter plot of SSA versus AE (or RRI versus AE, or dSSA versus AE). Based on their classifications, aerosols from ~~the~~ pure dust, polluted dust, biomass ~~-~~burning, industrial urban, developing urban, and marine ~~aerosols~~ sources (Figure 8 in Russell et al., 2014) can~~all could~~ be identified. For example~~: 1.~~, ~~The~~ the polluted dust aerosols ~~would be~~are mostly within the ellipses with smaller AE (near 1.0) values, relatively small~~er~~ SSA levels (0.85 to 0.95), ~~but~~ and much larger real refractive indices~~ex~~ (1.45 to 1.55) and SSA differences (0 to 0.05) than those present for~~compared with~~ other aerosols. ~~2.~~ The aerosols from ~~the~~ a developing urban area generally have smaller sizes than ~~the~~ polluted dust (AE ranging from 1 to 1.6), but they have larger SSA (0.9 to 1.0) values, ~~as well as~~ smaller real refractive indices~~ex~~ (1.4 to 1.5) and smaller SSA differences (~~around 0~~approximately 0). More classifications can be found in (Russell et al., 2014).~~3. The aerosols from the urban areas dominated by iIndustrial (UrbInd) development or those fromfrom biomass burning have the largest AE (exceeding 1.6) values. However, the UrbInd aerosols have much greaterlarger SSA values and SSA differences but have while smaller RRIreal refractive index values than compared with aerosols from biomass burning derived aerosols.~~ Based on their classification standards, the aerosols in urNJ could be basically ~~be~~ identified as ~~the~~ clusters of polluted dust, developing urban and industrial urban ~~kinds~~ during the sampling period, as shown in Figure 9, which further supports the analysis ~~in previous section~~in ~~the previous sections (~~Section 3~~)~~. ~~In the spring, dusts emitted from the desert regions in northern or to the north of China could be transported over a in long distant, arriving at theto YRD. During the transportation, trace gases or particles could be absorbed, which leads to and then a heterogeneous chemical reaction occurs. And . In addition, in other seasons, the aerosols are mostly derived from the local emissions within the urban areas and the nearby industrial areass around.~~

Although urNJ is only ~~about 3~~approximately 300-400 km ~~far~~ away from the East China Sea, few~~its aerosols are few composed by~~ marine or sea salt aerosol components are observed, as illustrated in Figure 9. Unfortunately,~~It is a pity that~~ the observations missed a biomass burning event in Jun 2012 (Zhuang et al., 2014b, 2015) because~~when~~ the instrument was having maintenance performed~~ained~~. Otherwise, the figure ~~will~~ would be more comprehensive. ~~This event was~~It's a very serious biomass burning episode, which directly resulteds in extremely high BC surface concentrations (6-7 times to the annual means, Zhuang et al., 2014b). Analysis here might ~~further~~ help us ~~to~~ understand the aerosol sources, transformations, transports and ~~its~~ radiative effects in the YRD. ~~And~~ . In addition, this information~~it~~ also indicates that the Mahalanobis Classification is a very useful approach for classifying ~~the~~ aerosol into types, especially in ~~the~~ cases of data shortages ~~of data~~ or insufficient ~~of~~ methods. However, ~~the~~ this method still has a limitation. The classified ellipses have some overlaps among different aerosols clusters. In overlap regions, ~~it's hard to further~~ ~~identify~~ classifying the aerosols into types is a challenge. For example, it is~~'s~~ not easy to distinguish between ~~the~~ polluted dust aerosols with large AE values ~~from the~~ and urban aerosols with smaller AE. Therefore, if there ~~were~~ are two kinds of aerosols with~~having~~ nearly identical coordinates, further information is needed, or a more effective approach~~es~~ should be taken into account.

Figure 9

In addition to the types, the aerosol mixtures/compositions can~~ould~~ also be identified based on SSA and AAOD. Generally, dust aerosols have~~s~~ strong absorption~~s~~ in the ultraviolet (UV) band~~,~~ but become non-absorbing in the visible band, leading to ~~its~~ SSAs increasing monotonically with the

wavelength ~~monotonically~~. For biomass burning aerosols, the~~its~~ SSAs ~~would~~ decrease monotonically with wavelength ~~monotonically~~. Non-monotonic~~ally~~ variations in SSA with changes ~~of the~~in wavelength might be due to aerosol mixtures dominated by ~~the other type~~ another type of aerosol ~~dominated mixtures~~, as indicated by Li et al. (2015c)~~,~~ ~~who~~ They ~~then~~ proposed two curvature parameters to provide additional information on the aerosol compositions:~~,~~ ~~defined as~~ the second derivative of the second-order polynomial fit of the SSA and wavelength and the fit of the AAOD and wavelength, as shown in Eq. 4 and Eq. 5~~, to provide additional information on the aerosol compositions~~.

$$\ln(SSA_\lambda) = \beta_2 \ln(\lambda)^2 + \beta_1 \ln(\lambda) + \beta_0 \quad (4)$$

$$\ln(AAOD_\lambda) = \alpha_2 \ln(\lambda)^2 + \alpha_1 \ln(\lambda) + \alpha_0 \quad (5)$$

~~Where,~~

where $-\beta_2$ and α_2 are the SSA c~~C~~urvature and AADO c~~C~~urvature, respectively. Detailed descriptions~~statements~~ ~~can~~ould ~~be found in~~were presented by Li et al. (2015c). Based on these parameters, the aerosols can~~ould~~ ~~basically~~ be identified as ~~the~~ dust dominated, BC~~black carbon~~ (including biomass burning and urban/industrial aerosols) dominated and other mixed (peak) type aerosols~~,~~ because the curvature probability (or frequency) distributions are different ~~among~~ for the different aerosol mixtures. As indicated in Li et al. (2015c), the SSA or AAOD c~~C~~urvature is mostly concentrated at ~~or around 0~~approximately 0 for the BC~~-~~-dominated aerosol mixture, which is much smaller than that of the dust~~-~~-dominated aerosol mixtures (0.1 for SSA c~~C~~urvature and 0.5-1 for AAOD c~~C~~urvature) over East Asia. Based on their method, the curvatures of SSA and AAOD are calculated and then divided into three categories according to the monotonicity of the SS~~A. ResultsA~~. The results show that there are ~~about 1~~approximately 15.0%, 27.5% and 42.3% occurrences of monotonically

increasing, decreasing and 670 nm peaking SSA spectrumsspectra, respectively, in urNJ. And . In addition, their probability (or frequency) distributions are plotted in Figure 10. Both the SSA and AAOD cCurvatures have substantial seasonalityies and are that is greatery, larger in colder seasons (not shown here). The figure indicates that the SSA and AAOD curvature patterns are highly consistent with those in Li et al. (2015c) for the monotonic categories, which impliesying that the there might be about 1approximately ~15% (mostly appearing in spring) and ~27% (mostly being in fall and winter) samples with monotonically increasing and decreasing SSA spectra occurrences ofare the dust-d-dominated and BC--dominated mixing aerosols, respectively, in urNJ during the observed period. For example, a very strong dust storm from northwest China and Mongolia on 1st May 2011 (Li et al., 2015a) directly yielded mean SSA and AAOD cCurvatures of 0.12 and 1.11, respectively, on 1st May 2011. These curvatures, which which are close to the values (0.11 and 1.24, respectively) of the pure dust aerosols (Li et al., 2015c). For the rest of the categoriesy with non-monotonic SSA spectraum, the SSA curvatures are mostly concentrated from 0.3 to 0.8, implying that the dust component might not exceed 10%, while the scattering species (organic carbon not included) at least accounteding for at least 30% within of the mixing particles in western YRD according to the sensitivitye results in from Li et al. (2015c). Subsidiary Additional data are needed to derive furtherif more information were going to be further identified. Results. However, these results here might help us gain ato better understanding of the mixings of the aerosols in the urban areas of the YRD. Similar to the work of Russell et al. (2014), Li et al. (2015c) also provideds an effective approach to for classifying the aerosol compositions based on a single data set (such as the CE-318 retrievals).

Figure 10

3.4 The direct radiative forcing of the aerosols

Based~~ing~~ on the abovementioned wavelength-~~-~~dependent optical properties ~~and~~ combined~~ing~~ with the observed surface albedo and aerosol profiles, the clear-~~-~~sky size-dependent ~~fractional~~ aerosol DRF~~direct radiative forcing (DRF)~~ of the fine and course ~~different~~ components at both the TOA~~top of atmosphere (TOA)~~ and the surface in urNJ are investigated using the~~a~~ radiation transfer model TUV (Madronich, 1993). Due to a lack of~~ing~~ SSA observations of each aerosol component, the scattering aerosol DRF is estimated based on a given SSA value (0.9999, ~~equaling~~equalling~~equal to~~ ~~to~~ that of sulfate or nitrate aerosol) in a reference ~~source~~ (Li et al., 2015b). As indicated in the last section, the absorbing aerosols in urNJ are always in a mixed state. Therefore, the absorbing aerosol DRF ~~is~~ cannot~~inappropriate to~~ be estimated directly using the BC SSA. Here, this value is~~it is~~ derived from the difference between the total and scattering aerosol DRFs, which might be more representative~~ness~~. ~~To make comparison~~For comparison, the aerosol DRF is also calculated based on the AAODs, AAEs and BC~~black carbon (BC)~~ SSA (Li et al., 2015b).

Observational~~Observed~~ aerosol profiles, which have not have been used in previous investigations (e~~.g.:~~.g.~~:~~, Zhuang et al., 2014a), might be important to the DRF~~s~~ estimations~~ng~~. Figure 11 shows the mean vertical aerosol profiles observed by CALIPSO (annual scale data) and the ~~Polarization Raman Lidar (~~PRL~~,~~ (seasonal scale data) in Nanjing. For further~~To make a~~ comparisons, all the profiles in the figure ~~have been~~were standardized to ~~a~~the percentages (%). ~~Similar to the AODs and AEs, t~~The figure suggests that the ground and satellite~~-based a~~-based aerosol profiles ~~also~~ are~~exist~~ substantially different~~ees~~. The CALIPSO profile is more homogeneous than the PRL one, accounting for ~~about 6~~approximately 61% and 88%, respectively, below 4 km. Due to the~~a~~ lack of the~~ing~~ long-term

measurement of PRL and the different products of the~~among~~ different observational platforms, both the CALIPSO and PRL profiles are used here. Additionally, a combined profile (~~gray~~grey line) of the ~~simply~~ averaged ~~between~~ CALIPSO and PRL values is included and~~. It~~ indicates that aerosols account for ~~about 7~~approximately 75% of the total~~s~~ below 4 km and ~~about 6~~approximately 60% in the boundary layer for the combined profile, which ~~to some extent~~ is somewhat similar to the default profile of TUV (Palancar and Toselli, 2004). All these four profiles were used when estimating the aerosol DRFs~~The aerosol DRFs would bewere estimated by TUV using all these four profiles~~.

Figure 11

3.4.1 The aerosol direct radiative forcing in clear~~-~~-sky conditions

Hereinafter, DRFs, unless otherwise specified, ~~hereinafter all~~ represent the averaged values ~~among~~ from CALIPSO, PRL and a combined profile ~~based f~~based forcing in clear~~-~~-sky conditions. Figure 12 shows the seasonal variations ~~of~~ in the size-dependent ~~fractional~~ daytime TOA and surface DRFs of the total, scattering and absorbing aerosols in urNJ. The aerosol DRFs are highly dependent~~ded~~ on the aerosol optical properties and compositions. Overall, the fine aerosols ~~have much more~~ contribute considerably more~~ions~~ to the total aerosol DRFs, especially for scattering aerosols. The coarse aerosol DRF ~~is~~ accounts for only ~~-15~~13.3% ~~of the fine aerosol DRF~~ for the scattering aerosols, while this fraction ~~accounts for~~ is ~~>51~~33.7% ~~of~~ for the~~for~~ absorbing aerosols at both the TOA and surface in urNJ. Negative scattering aerosol DRFs could be significantly offset at the TOA and could be ~~while~~ further strengthened at the surface by absorbing aerosols. Therefore, the total coarse aerosol DRF at the TOA is very weak due to a much smaller CSSA~~-~~ and~~-~~ subsequently~~-~~ accounts for a~~it has a~~ much smaller

contribution to the total aerosol DRF than the fine aerosols do. Both the scattering and absorbing aerosol DRFs have similar seasonality to their AODs~~, peaking in the summer for the total scattering aerosols and peaking while in the spring for the total absorbing aerosols. However, the DRF seasonal variations of for each aerosol type areis consistent with each other within the same mode, all peaking in the summer in the fine mode and peakingwhile in the spring in the coarse mode~~. And the scattering aerosol DRFs have the same seasonality as the absorbing ones within the same mode. In addition to AODs, the surface albedo and ~~the~~ solar zenith angle also have a strong influence on the variations ~~of~~ in the aerosol DRFs. As implied ~~in~~ by Zhuang et al. (2014a), a brighter surface would yield a weaker negative DRF ~~while~~ and a stronger positive DRF, assuming a ~~in the condition with~~ fixed AOD. The seasonal mean surface albedo averaged from four wavelengths (440, 670, 870 and 1020 nm) is ~~about~~ ~~0~~approximately 0.145, 0.170, 0.129, and 0.137 in the spring, summer, fall, and winter, respectively. ~~Therefore, the scattering aerosol DRF is stronger in the winter than in the spring, although SAOD is lower in the winter. Similarly, a stronger TOA DRF of the fine absorbing aerosols in the spring than in the winter might be also also be related to a higher surface albedo and solar zenith angles, although their AAODs in the winter are substantially higher. The weakest surface DRF appears in the spring for fine absorbing aerosols and in the summer for coarse absorbing aerosols, possibly due to thea higher surface albedo in this season.~~ As a result, the scattering and fine absorbing aerosol DRFs are also strong in the winter and spring, respectively.

——Unlike those of the single aerosol types, the variations of the total aerosol DRFs are co-affected by those of both the scattering and absorbing aerosols~~, meaning that the seasonal variations of in the TOA DRF are alsois additionally related to the SSAs' seasonality~~. Thus, the strongest TOA DRF of the total fine aerosols appears in the winter instead of the summer, and the total coarse aerosol DRFs are

positive at the TOA in the summer. For all modes, the seasonal variations of the total aerosol DRFs at the TOA are more consistent with thoseat of the fine mode. Compared withDifferent from the TOA DRFs of the total aerosols, the variations of the surface DRFs are much more consistent with those of the corresponding AODs and are, strongest in the summer and spring for the fine and coarse aerosols, respectivelyfine aerosols while in spring for coarse aerosols. The total aerosol DRFs at the surface are the strongest in the summer and weakest in the fall.

Figure 12

For furtherTo make comparisons (Figure 13), the absorbing aerosol DRFs based on the observed AAOD, AAE and fresh BC SSA (Li et al., 2015b) are also usedaccessed (named as the second way). Although the absorbing aerosol DRFs are estimated in different ways, they are highly correlated at both the TOA and surface, as shown in the figure. Apparently, the DRFs from the second method are much weaker than thoseat from the first calculation, one possibly due to the absorbing aerosols in urNJ being always in a constantly mixed state, as shown by the analysis in previous sectionin the previous section or and as indicated in by Zhuang et al. (2015). Jacobson (2000) suggesteds that the aged (mixed) absorbing aerosols have a much stronger abilitiesy ability to absorb solar radiation, withby a factor of two. Zhuang et al. (2013a and 2013b) stated that the simulated regional mean TOA DRF of the mixed BC (+1.56 W/m^2) over East Asia is about 1approximately 1.9 times to that of the noneun-mixed BC. And . Additionally, tThe ratio is about 1approximately 1.73 in this study, implying that the absorbing aerosol DRF from the first methodway is reasonable. The cComparison here further proves the importance of the mixing states into estimatinge the absorbing aerosol radiative effects.

Figure 13

Table 3 lists the annual mean size-dependent ~~fractional~~ DRFs of the total, scattering and absorbing aerosols at both the TOA and the surface in urNJ. The DRFs at the surface are all stronger than those at the TOA. The mean DRFs are -10.69, -16.45, 5.76 W/m^2 at the TOA and -25.54, -21.37 and -8.38 W/m^2 at the surface for the ~~total~~TA, ~~scattering~~ SA and ~~absorbing aerosols~~AA, respectively. The fine mode TOA DRFs ~~in fine mode~~ are nearly an order of magnitude stronger than those of the~~in~~ coarse mode for the total and scattering aerosols. The DRFs of the fine absorbing aerosols have the same order~~s~~ of magnitude ~~as,~~ but are stronger than those of the coarse absorbing aerosols. It's noting that the total DRFs in the table are not exactly the sum of the contributions from the fine and coarse ones, because the coarse aerosol affection on the solar radiation is excluded when calculating the fine aerosol DRF separately, and vice versa.

Table 3

Various studies of~~n the~~ aerosol DRFs have been carried out based on observations or numerical models. Over-all, the DRFs of urban aerosols are much stronger than those on ~~the~~ regional or global scales. Forster et al. (2007) summarized the global mean clear--sky DRFs of the total observational aerosols ~~from observations being~~as -5.4 W/m^2. Zhuang et al. (2013a and 2013b) indicated ~~a~~ that simulated clear--sky DRFs ~~being~~ are -4.97 W/m^2 for ~~the~~ total aerosols and ~~being~~while +1.2 W/m^2 for BC over East Asia. On a ~~sub-~~ subregional or urban scale, the observation~~ed based a~~-based analysis showed that the total aerosol DRFs always exceeded ~~at least~~ 10^1 W/m^2 (Markowicz et al., 2008; Khatri

et al., 2009; Wang et al., 2009; Kuhlmann and Quaas, 2010; Alam et al., 2011; Che et al., 2015c, and so on). For example, the total aerosol DRF could be as strong as -25 W/m^{2}over the Qinghai-Tibet Plateau (Kuhlmann and Quaas, 2010) and -30 W/m^2 in the north China Plain (Che et al., 2014 and 2015c)~~Kuhlmann and Quaas (2010) showed that the total aerosol DRFs wereas about -25 W/m^2 over the Qinghai-Tibet Plateau. Che et al. (2014; 2015c) indicated that the daytime total aerosol DRFs in northeastern China wereas about approximately -16.82 W/m^2 andwhile exceeded -30 W/m^2 in both the rural and urban areas of the north North China Plain duringin pollutioned episodes~~. Our results show that the aerosols in the urban area of the western YRD could also exert very strong DRFs, reaching as high as~~ as large as~~ -25.5 W/m^2 at the surface. Apparently, the DRFs here ~~would~~ have smaller uncertainties than those~~at~~ from simulations because of the use of observations. ~~Compared with the results in from Zhuang et al. (2014a), the DRFs here~~ And they might be also more precise compared with previous estimation in ~~because: 1. the observed aerosol profiles have not been used; and 2. the absorbed DRFs (which might be underestimated) were calculated using fresh BC SSA in by~~ Zhuang et al. (2014a). This study further investigate~~d~~s the size fractional ~~(fine and coarse)~~ DRFs of different aerosol components in urban areas of the western YRD, which ~~is in favor~~ allows a~~of~~ better understanding of the effects~~the acts~~ of aerosols ~~affecting~~ on solar shortwave ~~wave~~ radiation~~. And~~. In addition, these issues have not been addressed in previous ~~researches~~studies. The results here can~~ould~~ also be used to validate ~~the~~ numerical simulations and~~to~~ to evaluate ~~the~~ model performance~~s~~ concerning~~on the~~ aerosol radiative effects.

3.4.2 Sensitivity of the aerosol direct radiative forcing to aerosol profiles

Different aerosol profiles might result in different DRFs. Figure 14 presents the TOA and surface

DRFs of ~~the~~ different aerosol types, including the ~~scattering and~~SA, ~~absorbing aerosols~~AA and ~~the totals~~TA, based on four kinds of aerosol profiles from CALIPSO, PRL, the c~~C~~ombined CALIPSO and PRL shown in Figure 11 and~~as well as~~ the default one from~~in~~ TUV (Palancar and Toselli, 2004) in clear-~~-~~sky conditions. The figure shows that the aerosol DRFs in clear-~~-~~sky conditions ~~is~~ are not very sensitive to the aerosol profile~~s~~, although the absorbing aerosol TOA ~~-~~DRFs are more sensitive than those of the scattering aerosols. Overall, both the scattering and absorbing aerosol DRFs at the TOA ~~would~~ become weaker to some extent when~~if~~ more aerosols are~~were~~ concentrated in the lower layers of the atmosphere~~ or within the boundary layer~~, especially for the ~~latter case~~one~~AA~~'s. Here, a profile impact factor~~:~~ (PIF) is defined as the ratio of the standard deviations among the four types of DRFs in Figure 14 to the averaged values of~~among~~ these four DRFs. The PIF is ~~about 4~~approximately 4.97% for the absorbing aerosol TOA ~~-~~DRF and is~~while~~ below 2% for the rest of the types of DRFs~~, further proving the weak influence of the aerosol profiles on the clear- sky DRFs~~. In contrast, the aerosol profiles might have much stronger~~more~~ influences on the DRFs in cloudy sky conditions because the absorbing aerosols over brighter cloud will~~ould~~ absorb more short-wave radiation (Podgorny and Ramanathan, 2001). This issue ~~is~~ will ~~also going to~~ be addressed in the future~~rther~~.

Figure 14

3.4.3 Brief~~ly~~ discussions

Although the observation~~ based D~~-based DRFs of the total, scattering and absorbing aerosols~~,~~ as well as their sensitivities to the aerosol profiles are ~~analyzed~~ analysed in this study~~,~~; uncertainties still exist due to the measurement errors of the optical properties mentioned in Section 2. Additional

estimations of the aerosol DRFs are carried out based on the errors of AOD, AAOD and SSAs. Results. The results indicate that the greaterlarger uncertainties of the aerosol DRFs are mainly derived from the errors of SSA or AAOD. The uUncertainty of the total aerosol AODs (0.01) only yield only about 1approximately 1% relative biases for the total aerosol DRFs at both the TOA and surface. The total or fine aerosol SSA errors (0.03 or 0.037, respectively) may result in about 2approximately 24% of the uncertainties at the TOA (<15% at the surface) forto the corresponding DRFs. A larger coarse aerosol SSA error (0.085) leads to a ~ an ~24% uncertainties of its surface DRFs. AAOD errors (0.01) cause about 2approximately 20% of the uncertainties forto the absorbing DRFs at both the TOA and surface, while only accounting for only 1.2% ofto the scattering DRFs uncertainties. Overall, these uncertainties are relatively smaller than those presented in the 5th IPCC report (IPCC, 2013) and they could be further decreased if the measurements or the algorithms were fairlyfurther improved. In addition to the uncertainties, this study still findsexist limitations to be addressed in the future. FirstFor example, the absorbing aerosol DRFs would become more accurate if corresponding SSAs should could be further obtained by measurementsd in more detail to better estimate the corresponding DRFs. Second, the DRF would be a little more slightly more precise if the aAlso, the aerosol DRFs would be better estimated to a degree if its profiles with higher temporal resolutions could be were used instead of their annual means in future. Third, the long-term trends of the aerosol optical properties and their DRFdirect radiative forcing, including their interannual and interdecadal variations, should be taken into consideration. AdditionallyFinally, extremely high aerosol loadings are frequently observed duringin serious pollution episodes, including dust storms, biomass burning, and regional transport (Zhuang et al., 2014a, b and 2015). The aerosol optical and physical properties as well as the radiative forcing arewould be rather different duringin these extreme episodes, which also deserves further studyies.

4 Conclusions

In this study, the size-dependent ~~-dependentfractional~~ aerosol optical and physical properties observed by a Cimel sun photometer (CE-318), as well as the corresponding DRFs~~direct radiative forcing (DRF)~~ calculated by the~~a~~ radiation transfer model TUV based on observations from the~~in~~ urban area of Nanjing (urNJ), western YRD, are investigated.

In the urban area of the western YRD, the annual mean total aerosol AOD ~~at 550 nm~~ is 0.65~~, and~~ ~~is~~ and is mostly ~~contributed by the~~due to the contribution of the scattering components (0.61). The absorption fraction is as small as ~~about ~~ ~6.7%~~, changing with the seasons~~. A~~There are about 8~~pproximately 80% of the aerosols in urNJ during the sampling period are~~distributing in~~ fine mode aerosols ~~in urNJ during the sampling periods~~. The absorption fraction is ~~about 4~~approximately 4.6% in the fine mode and~~while~~ 15.5% in the coarse mode, showing the~~a~~ very different compositions and absorption characteristics of these two kinds of aerosols. Compared with the satellite retrievals, the observations show aerosol optical properties ~~here have~~ with much higher temporal resolutions and more products. Further analysis of~~n~~ the aerosol optical properties indicates that there might be ~~about 1~~approximately 15% and 27% occurrences of dust-~~-~~dominated and BC-~~-~~dominated mixing aerosols, respectively, in the western YRD during the study~~observed~~ period.

The aerosols in the western YRD have a two-mode lognormal pattern in their volume size distribution, peaking at the radi~~us~~ of 0.148 and 2.94 μm on an ~~in~~ annual scale. The fine particles have the same contribution as the coarse ones when AOD<0.8, and they become predominate when 0.8<AOD<1.4~~Both the fine and coarse particles makhavehave the same contributions to the totals at lower aerosol loadings (AOD<0.8). AtIn higher AOD (>0.8) levels, the fine aerosols are predominate.~~

794 ~~Results~~e. Different from observations in other regions, t~~T~~he results here further reveal~~indicate~~ that the

795 ~~fine or~~ coarse aerosols might also~~could~~ ~~individually~~ induce ~~a~~ very serious pollution~~ed~~ episodes in the

796 ~~urban region of the western~~ YRD. Both ~~the~~ fine and coarse aerosols have the same levels of volume

797 concentrations, although their radii~~uses~~ differ by an order of magnitude.

798 ~~The mean DRF of the total aerosols is -10.69 W/m^2 at the TOA and -25.54 W/m^2 at the surface, in~~

799 ~~clear- sky conditions~~Similar to AODs,~~.~~ t~~T~~he total fine aerosol DRF also have a much contribution to

800 the totals, especially at TOA (>~~accounts for more than~~ 97%~~) of the totals at the TOA~~, with a value of

801 -11.17 W/m^2. However, differences exist. For each aerosol type, ~~Estimations of~~n ~~the size-dependent~~

802 ~~dependentfractional DRFs of each aerosol component indicate that~~ the coarse aerosol DRF accounts~~is~~

803 for only ~13.3~~5~~% for the scattering aerosols while at least 33.7% for the absorbing aerosols~~of the fine~~

804 ~~one within the scattering aerosols and iswhile >51% within absorbing aerosols~~ at both the TOA and the

805 surface in urNJ. The DRFs estimated for urNJ in this study are much stronger than their regional or

806 global means.

807 Most of t~~T~~he size-dependent ~~dependentfractional~~ aerosol optical and~~,~~ physical properties as well

808 as their~~nd~~ DRFs have significant seasonality in the western YRD. The DRF variations ~~of~~ for each

809 aerosol type within the same mode are mostly consistent with the variations ~~of~~~~of~~in the corresponding

810 AODs, ~~all~~ peaking in the summer for the fine aerosols and~~while~~ in the spring for the coarse ones.

811 However, the variations ~~of~~ in the total aerosol DRFs at the TOA are different from the corresponding

812 AODs ~~within the same size segment~~ because the negative DRFs of the scattering aerosols are always

813 offset by the absorbing aerosols. Both the fine and coarse aerosols have the largest sizes ~~and are the~~

814 ~~most absorbing~~ in the summer, which ~~are~~ differs~~ent~~ from the total~~whole mode~~ aerosol mode~~s~~ (which

815 peaks in the spring).

The sensitivities of clear--sky aerosol DRFs to the aerosol profiles are not significant and are, all smaller than 5%. Overall, both the scattering and absorbing aerosol DRFs at the TOA would become a somewhat little weaker to some extent if more aerosols arewerewere concentrated in the lower layers of the atmosphere, especially for the absorbed DRF. Further investigation suggests that another uncertainty of the DRFs is from the measuring errors of the aerosol optical properties. The lL arger biases are mainly derived from the errors of the SSA and AAOD.

Acknowledgements: This work was supported by the National Key R&DBasic Research Development Program of China (2017YFC0209803, 2014CB441203, 2016YFC0203303), the National Natural Science Foundation of China (41675143, 91544230, 41621005), and a project Funded by the Priority Academic Program Development of the Jiangsu Higher Education Institutions (PAPD). The authors would like to thank all members in the AERC of Nanjing University for maintaining instruments, and also thank the anonymous reviewers for their constructive and valuable comments on this paper.

5 References

Alam, K., Trautmann, T., and Blaschke, T.: Aerosol optical properties and radiative forcing over mega-city Karachi. Atmos. Res. 101, 773-782, 2011.

Angström, A.: On the atmospheric transmission of sun radiation and on dust in the air, Geogr. Ann., 11, 156–166, 1929.

Arnott, W. P., Hamasha, K., Moosmuller, H., Sheridan, P. J., and Ogren, J. A.: Towards aerosol light-absorption measurements with a 7-wavelength aethalometer: evaluation with a photoacoustic instrument and 3-wavelength nephelometer, Aerosol Sci. Tech., 39, 17–29,

838 doi:10.1080/027868290901972, 2005.
839 Bellouin, N., Boucher, O., Tanré, D., and Dubovik, O.: Aerosol absorption over the clear-sky oceans
840 deduced from POLDER-1 and AERONET observations, Geophys. Res. Lett., 30, 1748,
841 doi:10.1029/2003GL017121, 2003.
842 Bergin, M. H., Cass, G. R., Xu, J., Fang, C., Zeng, L., Yu, T., Salmon, L. G., Kiang, C. S., Tang, X. Y.,
843 Zhang, Y. H., and Chameides, W. L.: Aerosol radiative, physical, and chemical properties in Beijing
844 during June 1999, J. Geophys. Res., 106 (D16), 17969–17980, 2001.
845 Cai, H. K., Zhou, R. J., Fu, Y. F., Zheng, Y. Y., and Wang, Y. J.: Cloud-aerosol lidar with or thogonal
846 polarization detection of aerosol optical properties after a crop burning case, Clim. Environ. Res.,
847 16, 469–478, 2011.
848 Che, H. Z., Zhang, X. Y., Xia, X., Goloub, P., Holben, B., Zhao, H., Wang, Y., Zhang, X. C., Wang, H.,
849 Blarel, L., Damiri, B., Zhang, R., Deng, X., Ma, Y., Wang, T., Geng, F., Qi, B., Zhu, J., Yu, J., Chen,
850 Q., and Shi, G..: Ground-based aerosol climatology of China: aerosol optical depths from the China
851 Aerosol Remote Sensing Network (CARSNET) 2002–2013, Atmos. Chem. Phys., 15, 7619–7652,
852 2015a.
853 Che, H. Z., Zhao, H. J., Wu, Y. F., Xia, X. A., Zhu, J., Wang, H., Wang, Y. Q., Sun, J. Y., Yu, J., Zhang,
854 X. Y., and Shi, G. Y.: Analyses of aerosol optical properties and direct radiative forcing over urban
855 and industrial regions in Northeast China, Meteorology and Atmospheric Physics, 127(3), 345-354,
856 doi:10.1007/s00703-015-0367-3, 2015c.
857 Che, H., Wang, Y., and Sun, J.: Aerosol optical properties at Mt. Waliguan observatory, China, Atmos.
858 Environ., 45, 6004–6009, 2011.
859 Che, H., Xia, X., Zhu, J., Li, Z., Dubovik, O., Holben, B., Goloub, P., Chen, H., Estelles, V.,

Cuevas-Agulló, E., Blarel, L., Wang, H., Zhao, H., Zhang, X., Wang, Y., Sun, J., Tao, R., Zhang, X., and Shi, G.: Column aerosol optical properties and aerosol radiative forcing during a serious haze-fog month over North China Plain in 2013 based on ground-based sunphotometer measurements, Atmos. Chem. Phys., 14, 2125–2138, doi:10.5194/acp-14-2125-2014, 2014.

Che, H., Xia, X., Zhu, J., Wang, H., Wang, Y., Sun, J., Zhang, X., and Shi, G.: Aerosol optical properties under the condition of heavy haze over an urban site of Beijing, China, Environ. Sci. Pollut. R., 22, 1043–1053, doi:10.1007/s11356-014-3415-5, 2015b.

Che, H.,Wang, Y., Sun, J., Zhang, X., Zhang, X., and Guo, J.: Variation of Aerosol Optical Properties over the Taklimakan Desert in China, Aerosol Air Qual. Res., 13, 777–785, 2013.

Chiang, C. W., Chen, W. N., Liang, W. A., Das, S. K., and Nee, J. B.: Optical properties of tropospheric aerosols based on measurements of lidar, sun-photometer, and visibility at Chung-Li (25^{o}N, 121^{o}E), Atmos. Environ., 41, 4128-4137, doi:10.1016/j.atmosenv.2007.01.019, 2007.

Deng, J. J., Zhang, Y. R., Hong, Y. W., Xu, L. L., Chen, Y. T., Du, W. J., and Chen, J. S.: Optical properties of $PM_{2.5}$ and the impacts of chemical compositions in the coastal city Xiamen in China, Science of the Total Environment, 557-558, 665-675, 2016.

Dong, Z. P., Li, X. M., Du, C. L., and, Zhang, G. J.: Study on aerosol optical property in Xi'An Region, Plateau Meteorology, 32(3), 856-864, doi:10.7522/j.issn.1000-0534.2012.00079, 2013.

Dubovik, O. and King, M. D.: A flexible inversion algorithm for the retrieval of aerosol optical properties from Sun and sky radiance measurements, J. Geophys. Res., 105, 20673–20696, doi:10.1029/2000JD900282, 2000.

Dubovik, O., Sinyuk, A., Lapyonok, T., Holben, B. N., Mishchenko, M., Yang, P., Eck, T. F., Volten, H., Munoz, O., Veihelmann, B., van der Zande, W. J., Leon, J. F., Sorokin, M., and Slutsker, I.:

882 Application of spheroid models to account for aerosol particle nonsphericity in remote sensing of
883 desert dust, J. Geophys. Res.-Atmos., 111, D11208, doi:10.1029/2005jd006619, 2006.
884 Fan, X. H., Chen, H. B., Xia, X. A., Li, Z. Q., and Cribb, M.: Aerosol optical properties from the
885 Atmospheric Radiation Measurement Mobile Facility at Shouxian. China, J. Geophys. Res., 115,
886 D00K33, doi:10.1029/2010JD014650, 2010.
887 Forster, P., Ramaswamy, V., Artaxo, P., Berntsen, T., Betts, R., Fahey, D. W., Haywood, J., Lean, J.,
888 Lowe, D. C., Myhre, G., Nganga, J., Prinn, R., Raga, G., Schulz, M., and Van Dorland, R.: Changes
889 in atmospheric constituents and in radiative forcing, in: Climate Change 2007: The Physical
890 Science Basis. Contribution of Working Group I to the Fourth Assessment Report of the
891 Intergovernmental Panel on Climate Change, edited by: Solomon, S. et al., Cambridge Univ. Press,
892 Cambridge, UK, 129–234, 2007.
893 Hansen, A. D. A., Rosen, H., and Novakov, T.: The aethalometer: an instrument for the real time
894 measurements of optical absorption by aerosol particles, Sci. Total Environ., 36, 191–196, 1984.
895 He, X., Li, C. C., Lau, A. K. H., Deng, Z. Z., Mao, J. T., Wang, M. H., and Liu, X. Y.: An intensive
896 study of aerosol optical properties in Beijing urban area, Atmos. Chem. Phys., 9, 8903–8915,
897 doi:10.5194/acp-9-8903-2009, 2009.
898 Holben, B. N., Eck, T. F., Slutsker, I., Tanre, D., Buis, J. P., Setzer, A., Vermote, E., Reagan, J. A.,
899 Kaufman, Y. J., Nakajima, T., Lavenu, F., Jankowiak, I., and Smirnov, A.: AERONET-a federated
900 instrument network and data archive for aerosol characterization, Remote Sens. Environ., 66, 1-16,
901 1998.
902 Holler, R., Ito, K., Tohno, S., and Kasahara, M.: Wavelength-dependent aerosol single scattering albedo:
903 measurements and model calculations for a coastal site near the sea of Japan during ACE-Asia, J.

Geophys. Res., 108, 8648, doi:10.1029/2002JD003250, 2003.

IPCC 2013: Climate Change 2013: The Physical Science Basis. Contribution of Working Group I to the Fifth Assessment Report of the Intergovernmental Panel on Climate Change, edited by: Stocker, T. F., Qin, D., Plattner, G.-K., Tignor, M., Allen, S. K., Boschung, J., Nauels, A., Xia, Y., Bex, V., and Midgley, P. M., Cambridge University Press, Cambridge, UK and New York, NY, USA, 1535 pp., 2013.

Jacobson, M. Z.: A physically based treatment of elemental carbon optics: implication for global direct forcing of aerosols, Geophys. Res. Lett., 27, 217-220, 2000.

Jacobson, M. Z.: Control of fossil-fuel particulate black carbon and organic matter, possibly the most effective method of slowing global warming, J. Geophys. Res., 107, 4410, doi:10.1029/2001JD001376, 2002.

Jiang, Z., Liu, Z., Wang, T., Schwartz, C. S., Lin, H.-C., and Jiang, F.: Probing into the impact of 3DVAR assimilation of surface PM_{10} observations over China using process analysis, J. Geophys. Res. Atmos., 118, 6738–6749, doi:10.1002/jgrd.50495, 2013.

Khatri, P., Ishizaka, Y., and Takamura, T.: A study on aerosol optical properties in an urban atmosphere of Nagoya, Japan. J. Meteorol. Soc. Jpn., 87 (1), 19-38, 2009.

Kiehl, J. T. and Briegleb, B. P.: The relative roles of sulfate aerosols and greenhouse gases in climate forcing, Science, 260, 311–314, 1993.

Kuhlmann, J., and Quaas, J.: How can aerosols affect the Asian summer monsoon? Assessment during three consecutive pre-monsoon seasons from CALIPSO satellite data, Atmos. Chem. Phys., 10, 4673-4688, doi:10.5194/acp-10-4673-2010, 2010.

Li, J., Carlson, B. E., and Lacis, A. A.: Using single-scattering albedo spectral curvature to characterize

East Asian aerosol mixtures, J. Geophys. Res. Atmos., 120, 2037–2052, 2015c.

Li, J., Wang, W.-C., Liao, H., and Chang, W. Y.: Past and future direct radiative forcing of nitrate aerosol in East Asia, Theor. Appl. Climatol., 121, 445–458, 2015b.

Li, S., Wang, T. J., Xie, M., Han, Y., and Zhuang, B. L.: Observed aerosol optical depth and angstrom exponent in urban area of Nanjing, China, Atmos. Environ., 123, 350-356, doi:10.1016/j.atmosenv.2015.02.048, 2015a.

Liao, H. and Seinfeld, J. H.: Global impacts of gas-phase chemistry-aerosol interactions on direct radiative forcing by anthropogenic aerosols and ozone, J. Geophys. Res., 110, D18208, doi:10.1029/2005JD005907, 2005.

Ma, X. X., Liu, H. N., Liu, J., and Zhuang, B. L.: Sensitivity of climate effects of black carbon in China to its size distributions, Atmospheric Research, 185, 118-130, 2017.

Ma, X., and Yu, F.: Effect of spectral dependent surface albedo on Saharan dust direct radiative forcing. Geophys. Res. Lett. 39, L09808, 2012.Madronich, S.: UV radiation in the natural and perturbed atmosphere, In: Tevini,M. (Ed.), UV-B Radiation and Ozone Depletion, Effects on Humans, Animals, Plants, Microorganisms, and Materials, Lewis Publisher, Boca Raton, pp. 17-69, 1993.

Markowicz, K. M., Flatau, P. J., Remiszewska, J., Witek, M., Reid, E. A., Reid, J. S., Bucholtz, Z., and Hilben, B.: Observations and modeling of the surface aerosol radiative forcing during UAE. J. Atmos. Sci. 65, 2877-2891, 2008.

Menon, S., Hansen, J., Nazarenko, L., and Luo, Y. F.: Climate effects of black carbon aerosols in China and India, Science, 297, 2250–2253, doi:10.1126/science.1075159, 2002.

Palancar, G.G., and Toselli, B. M.: Effects of meteorology and tropospheric aerosols on UV-B radiation: a 4-year study. Atmos. Environ. 18, 2749-2757, 2004.

948 Pan, L, Che, H. Z., Geng, F. H., Xia, X. A., Wang, Y. Q., Zhu, C. Z., Chen, M., Gao, W., and Guo, J. P.:
949 Aerosol optical properties based on ground measurements over the Chinese Yangtze Delta Region,
950 Atmos. Environ., 44, 2587-2596, doi:10.1016/j.atmosenv.2010.04.013, 2010.
951 Peng, Z., Liu, Z. Q., Chen, D., and Ban, J. M: Improving PM2:5 forecast over China by the joint
952 adjustment of initial conditions and source emissions with an ensemble Kalman filter, Atmos. Chem.
953 Phys., 17, 4837–4855, 2017.
954 Penner, J. E., Andreae, M., Annegarn, H., Barrie, L., Feichter, J., Hegg, D., Jayaraman, A., Leaitch, R.,
955 Murphy, D., Nganga, J., and Pitari, G.: Aerosols, their direct and indirect effects, in: Climate
956 Change 2001: The Scientific Basis. Contribution of Working Group I to the Third Assessment
957 Report of the Intergovernmental Panel on Climate Change, edited by: Houghton, J. T. et al.,
958 Cambridge University Press, Cambridge, UK and New York, NY, USA, 289–348, 2001.
959 Podgorny, I. A., and Ramanathan, V.: A modeling study of the direct effect of aerosols over the
960 tropical Indian Ocean, J Geophys. Res. 106, D20, 24097–24105, 2001.
961 Qi, B., Hu, D. Y., Che, H. Z., Du, R. G., Wu, Y. F., Xia, X. A., Zha, B., Liu, J., Niu, Y. W., Wang, H.,
962 Zhang, X. Y., and Shi, G. Y.: Seasonal variation of aerosol optical properties in an urban site of the
963 Yangtze Delta Region of China. Aerosol Air Qual. Res., 16, 2884-2896, 2016.
964 Reddy, M. S., Boucher, O., Bellouin, N., Schulz, M., Balkanski, Y., Dufresne, J. L., and Pham, M.:
965 Estimates of global multicomponent aerosol optical depth and direct radiative perturbation in the
966 Laboratoire de Meteorologie Dynamique general circulation model, J. Geophys. Res., 110, D10S16,
967 doi:10.1029/2004JD004757, 2005.
968 Russell, P. B., Kacenelenbogen, M., Livingston, J. M., Hasekamp, O. P., Burton, S. P., Schuster, G. L.,
969 Johnson, M. S., Knobelspiesse, K. D., Redemann, J., Ramachandran, S., and Holben, B.: A

multiparameter aerosol classification method and its application to retrievals from spaceborne polarimetry, J. Geophys. Res.-Atmos., 119, 9838–9863, doi:10.1002/2013JD021411, 2014.

Sun, H., Pan, Z., and Liu, X.: Numerical simulation of spatial-temporal distribution of dust aerosol and its direct radiative effects on East Asian climate, J. Geophys. Res., 117, D13206, doi:10.1029/2011JD017219, 2012.

Tao, R., Che, H. Z., Chen, Q. L., Tao, J., Wang, Y. Q., Sun, J. Y., Wang, H., and Zhang, X. X.: Study of aerosol optical properties based on ground measurements over Sichuan Basin, China, Aerosol and Air Quality Research, 14: 905–915. doi:10.4209/aaqr.2012.07.0200, 2014.

Wang, T. J., Zhuang, B. L., Li, S., Liu, J., Xie, M., Yin, C. Q., Zhang, Y., Yuan, C., Zhu, J. L., Ji, L. Q., and Han, Y.: The interactions between anthropogenic aerosols and the East Asian summer monsoon using RegCCMS, J. Geophys. Res. Atmos., 120, doi:10.1002/2014JD022877, 2015.

Wang, Y., Che, H. Z., Ma, J. Z., Wang, Q., Shi, G. Y., Chen, H. B., Goloub, P., and Hao, X. J.: Aerosol radiative forcing under clear, hazy, foggy, and dusty weather conditions over Beijing, China, Geophys. Res. Lett., 36, L06804, doi:10.1029/2009GL037181, 2009.

Weingartner, E., Saathoff, H., Schnaiter, M., Streit, N., Bitnar, B., and Baltensperger, U.: Absorption of light by soot particles: determination of the absorption coefficient by means of aethalometers, J. Aerosol Sci., 34, 1445–1463, doi:10.1016/S0021-8502(03)00359-8, 2003.

Wu, Y. F., Zhang, R. J., Pu, Y. F., Zhang, L. M., Ho, K. F., and Fu, C. B.: Aerosol optical properties observed at a semi-arid rural site in northeastern China, Aerosol Air Qual. Res., 12, 503–514, 2012.

Xia, X. A., Li, Z. Q., Holben, B., Wang, P., Eck, T., Chen, H. B., Cribb, M., and Zhao, Y. X.: Aerosol optical properties and radiative effects in the Yangtze Delta region of China, J. Geophys. Res., 112, D22S12, doi:10.1029/2007JD008859, 2007.

992 Xia, X., Che, H., Zhu, J., Chen, H., Cong, Z., Deng, X., Fan, X., Fu, Y., Goloub, P., Jiang, H., Liu, Q.,
993 Mai, B., Wang, P., Wu, Y., Zhang, J., Zhang, R., and Zhang, X.: Ground-based remote sensing of
994 aerosol climatology in China: aerosol optical properties, direct radiative effect and is
995 parameterization, Atmos. Environ., 214, 243-251, doi:10.1016/j.atmosenv.2015.06.071, 2016.
996 Xu, J., Bergin, M. H., Greenwald, R., Schauer, J. J., Shafer, M. M., Jaffrezo, J. L., and Aymoz, G.:
997 Aerosol chemical, physical, and radiative characteristics near a desert source region of Northwest
998 China during ACE-Asia, J. Geophys. Res., 109, D19S03, doi:10.1029/2003JD004239, 2004.
999 Xu, J., Bergin, M. H., Yu, X., Liu, G., Zhao, J., Carrico, C. M., and Baumann, K.: Measurement of
1000 aerosol chemical, physical and radiative properties in the Yangtze delta region of China, Atmos.
1001 Environ., 36, 161–173, 2002.
1002 Xu, J., Tao, J., Zhang, R., Cheng, T., Leng, C., Chen, J., Huang, G., Li, X., and Zhu, Z.: Measurements
1003 of surface aerosol optical properties in winter of Shanghai, Atmos. Res., 109-110, 25–35, 2012.
1004 Xu, X.: Retrieval of aerosol microphysical properties from AERONET photolarimetric measurements.
1005 PhD diss., Department of Earth and Atmospheric Sciences, University of Nebraska-Lincoln, 2015.
1006 Yan, P., Tang, J., Huang, J., Mao, J. T., Zhou, X.J., Liu, Q., Wang, Z. F., and Zhou, H. G.: The
1007 measurement of aerosol optical properties at a rural site in Northern China, Atmos. Chem. Phys., 8,
1008 2229–2242, doi:10.5194/acp-8-2229-2008, 2008.
1009 Yu, J., Che, H. Z., Chen, Q. L., Xia, X. A., Zhao, H. J., Wang, H., Wang, Y. Q., Zhang, X. X., and Shi,
1010 G. Y.: Investigation of aerosol optical depth (AOD) and Ångström exponent over the desert region
1011 of northwestern China based on measurements from the China Aerosol Remote Sensing Network
1012 (CARSNET), Aerosol Air Qual. Res., 15, 2024-2036, doi:10.4209/aaqr.2014.12.0326, 2015.
1013 Yu, X. N., Ma, J., Kumar, K. R., Zhu, B., An, J. L., He, J. Q., and Li, M.: Measurement and analysis of

surface aerosol optical properties over urban Nanjing in the Chinese Yangtze River Delta, Sci. Total Environ., 542, 277-291, 2016.

Yu, X. N., Zhu, B., Yin, Y., Fan, S. X., and Chen, A. J.: Seasonal variation of columnar aerosol optical properties in Yangtze River Delta in China, Adv. Atmos. Sci., 28(6), 1326-1335, doi:10.1007/s00376-011-0158-9, 2011.

Zhang, L., Sun, J. Y., Shen, X. J., Zhang, Y. M., Che, H., Ma, L. Q., Zhang, Y. W., Zhang, X. Y., and Ogren, J. A.: Observations of relative humidity effects on aerosol light scattering in the Yangtze River Delta of China, Atmos. Chem. Phys., 15, 8439–8454, 2015.

Zhang, Q., Streets, D. G., Carmichael, G. R., He, K. B., Huo, H., Kannari, A., Klimont, Z., Park, I. S., Reddy, S., Fu, J. S., Chen, D., Duan, L., Lei, Y., Wang, L. T., and Yao, Z. L.: Asian emissions in 2006 for the NASA INTEX-B mission, Atmos. Chem. Phys., 9, 5131–5153, doi:10.5194/acp-9-5131-2009, 2009.

Zhang, W., Hu, B., Chen, C. H., Du, P., Zhang, L., and Feng, G. H.: Scattering properties of atmospheric aerosols over Lanzhou City and applications using an integrating nephelometer, Adv. Atmos. Sci., 21(6), 848–856, 2004.

Zhang, X. Y., Wang, Y. Q., Niu, T., Zhang, X. C., Gong, S. L., Zhang, Y. M., and Sun, J. Y.: Atmospheric aerosol compositions in China: Spatial/temporal variability, chemical signature, regional haze distribution and comparisons with global aerosols, Atmos. Chem. Phys., 12, 779–799, doi:10.5194/acp-12-779-2012, 2012.

Zhao, H. J., Che, H. Z., Zhang, X. Y., Ma, Y. J., Wang, Y. F., Wang, X. X., Liu, C., Hou, B., and Che, X. C.: Aerosol optical properties over urban and industrial region of Northeast China by using ground-based sun-photometer Measurement, Atmos. Environ., 75, 270-278.

1036 doi:10.1016/j.atmosenv.2013.04.048, 2013.

1037 Zheng, Y., Che, H. Z., Zhao, T. L., Xia, X. A., Gui, K., An, L. C., Qi, B., Wang, H., Wang, Y. Q., Yu, J.,
1038 and Zhang, X. Y.: Aerosol optical properties during the World Athletics Championships and Victory
1039 Day Military Parade over Beijing in August and September 2015, Atmosphere, 7(3), 47;
1040 doi:10.3390/ atmos7030047, 2016.

1041 Zhu, J., Che, H. Z., Xia, X. A., Chen, H. B., Goloub, P., and Zhang, W. X.: Column-integrated aerosol
1042 optical and physical properties at a regional background atmosphere in North China Plain, Atmos.
1043 Environ., 84, 54-64, doi:10.1016/j.atmosenv.2013.11.019, 2014.

1044 Zhu, J., Wang, T., Talbot, R., Mao, H., Hall, C. B., Yang, X., Fu, C., Zhuang, B., Li, S., Han, Y., and
1045 Huang, X.: Characteristics of atmospheric Total Gaseous Mercury (TGM) observed in urban
1046 Nanjing, China, Atmos. Chem. Phys., 12, 12103–12118, doi:10.5194/acp-12-12103-2012, 2012.

1047 Zhuang, B. L., Li, S., Wang, T. J., Deng, J. J., Xie, M., Yin, C. Q., and Zhu, J. L.: Direct radiative
1048 forcing and climate effects of anthropogenic aerosols with different mixing states over China,
1049 Atmos. Environ., 79, 349–361, doi:10.1016/j.atmosenv.2013.07.004, 2013a.

1050 Zhuang, B. L., Liu, Q., Wang, T. J., Yin, C. Q., Li, S., Xie, M., Jiang, F., and Mao, H. T.: Investigation
1051 on semi-direct and indirect climate effects of fossil fuel black carbon aerosol over China, Theor.
1052 Appl. Climatol., 114, 651–672, doi:10.1007/s00704-013-0862-8, 2013b.

1053 Zhuang, B. L., Wang, T. J., Li, S., Liu, J., Talbot, R., Mao, H. T., Yang, X. Q., Fu, C. B., Yin, C. Q.,
1054 Zhu, J. L., Che, H. Z., and Zhang, X. Y.: Optical properties and radiative forcing of urban aerosols
1055 in Nanjing, China, Atmos. Environ., 83, 43–52, 2014a.

1056 Zhuang, B. L., Wang, T. J., Liu, J., Li, S., Xie, M., Han, Y., Chen, P. L., Hu, Q. D., Yang, X. Q., Fu, C.
1057 B., Zhu, J. L.: The surface aerosol optical properties in urban area of Nanjing, west Yangtze River

Delta, China, Atmos. Chem. Phys., 17, 1143–1160, 2017.

Zhuang, B. L., Wang, T. J., Liu, J., Li, S., Xie, M., Yang, X. Q., Fu, C. B., Sun, J. N., Yin, C. Q., Liao, J. B., Zhu, J. L., and Zhang, Y.: Continuous measurement of black carbon aerosol in urban Nanjing of Yangtze River Delta, China, Atmos. Environ., 89, 415–424, 2014b.

Zhuang, B. L., Wang, T. J., Liu, J., Ma, Y., Yin, C. Q., Li, S., Xie, M., Han, Y., Zhu, J. L., Yang, X. Q., and Fu, C. B.: Absorption coefficient of urban aerosol in Nanjing, west Yangtze River Delta, China, Atmos. Chem. Phys., 15, 13633–13646, 2015.

Figure captions:

Figure 1. Monthly variations of the total (a), scattering (b), and absorbing (c) aerosol optical depths (AOD) at 550 nm, including the ratio of the AOD in fine or coarse mode to the AOD in all mode (line with triangle markers in green) in urban area of Nanjing. The 10th, 25th, median, 75th, 90th percentile values of the all mode AOD are presented as box plots. The monthly means of the all mode AODs are presented as cycle markers in gray.

Figure 2. Monthly variations of the total (a), scattering (b), and absorbing aerosol (c) Ångström exponents (AE) at 440/870 nm for the all, fine and coarse modes in urban area of Nanjing.

Figure 3. Monthly variations of the all, fine, and coarse mode aerosol single scattering albedo (SSA) at 550 nm (a) and the aerosol refractive indices at 440 nm (b) in urban area of Nanjing.

Figure 4. Frequency distributions of the size dependent AODs at 550 nm (a), AEs at 440/870 nm (b), SSAs at 550 nm (c) as well as the real and imaginary parts at 440 nm (c) in urban area of Nanjing.

Figure 5. Comparisons between CE-318 and MODIS based AOD at 550 nm and between AE at 440/870 nm for CE-318 and at 412/470 nm for MODIS in Nanjing.

1080 Figure 6. Comparisons between the absorbing aerosol optical depth (AAOD) at 550 nm from CE-318
1081 and surface absorption coefficient (AAC) at 520 nm from AE-31 (a) and between the column AAE at
1082 440/870 nm from CE-318 and surface AAE at 470/880 nm from AE-31 (b) in urban Nanjing.
1083 Figure 7. The averaged aerosol volume size ($\mu m^3/\mu m^2$) distributions in different seasons (a) and in
1084 different AOD levels in urban Nanjing.
1085 Figure 8. Seasonal variations of the effective (a, μm) and mean (b, μm) radius of aerosols as well as the
1086 aerosol volume concentrations (c, $\mu m^3/cm^3$) in the all, fine and coarse modes in urban Nanjing.
1087 Figure 9. Relationships between the monthly mean values of 491 nm SSA and total Ångström exponent
1088 (AE) at 491/870 nm (a), between the monthly mean values of the real refractive index at 670 nm and
1089 AE at 491/870 nm (b), and between the monthly mean values of the SSA difference (870–491 nm) and
1090 AE at 491/870 nm (c).
1091 Figure 10. Distribution of the SSA and AAOD Curvatures in urban area of Nanjing under different
1092 spectral SSA conditions, including monotonically decreasing, increasing SSA spectra and peaked SSA
1093 spectra.
1094 Figure 11. The aerosol vertical proportions (%) from CALIPSO, Polarization-Raman Lidar and their
1095 average in Nanjing.
1096 Figure 12. Seasonal variations of the clear sky aerosol direct radiative forcing (DRF, W/m^2) at both
1097 TOA (a~c) and the surface (d~f). The DRFs of the total (a, d), scattering (b, e) and absorbing (c, f)
1098 aerosols in the all, fine and coarse modes are all investigated in urban Nanjing.
1099 Figure 13. Comparisons in the absorbing aerosol DRFs (W/m^2) between from BC SSA and from the
1100 total aerosol DRF minus the scattering one.
1101 Figure 14. Sensitivities of the TOA and the surface aerosol DRFs (day time, W/m^2) to the different

aerosol profiles in clear conditions, for the total, scattering and absorbing aerosols.

Tables:

Table 1 Statistical summary of the columnar aerosol optical properties in urban area of Nanjing

Factors	Max	Min	Mean±SD	Meadian
550 nm AOD	2.3208	0.2723	0.6494±0.2852	0.5912
550 nm FAOD	2.2216	0.1468	0.5257±0.2806	0.4479
550 nm CAOD	0.9891	0.0139	0.1237±0.1076	0.0858
550 nm SAOD	2.2744	0.2443	0.6059±0.2747	0.5492
550 nm FSAOD	2.1459	0.1435	0.5014±0.2713	0.4263
550 nm CSAOD	0.8842	0.0113	0.1045±0.0957	0.0705
550 nm AAOD	0.2304	0.0020	0.0435±0.0240	0.0421
550 nm FAAOD	0.1424	0.0005	0.0244±0.0175	0.0208
550 nm CAAOD	0.1163	0.0009	0.0192±0.0145	0.0156
440/870 nm AE	1.9100	0.3085	1.2045±0.2856	1.2436
440/870 nm FAE	2.3625	0.3565	1.7083±0.2979	1.7364
440/870 nm CAE	-0.0789	-0.3805	-0.1876±0.0430	-0.1898
440/870 nm SAE	1.9916	0.2958	1.1976±0.3085	1.2386
440/870 nm FSAE	2.3653	0.3463	1.7102±0.2980	1.7368
440/870 nm CSAE	-0.1048	-0.7111	-0.3838±0.1017	-0.3864
440/870 nm AAE	3.4619	0.1483	1.3237±0.4820	1.2587
440/870 nm FAAE	4.5118	0.2912	1.7521±0.6470	1.6516
440/870 nm CAAE	3.1264	-0.0844	0.8748±0.4589	0.8209
550 nm SSA	0.9959	0.8053	0.9297±0.0335	0.9305
550 nm FSSA	0.9974	0.8388	0.9524±0.0261	0.9549
550 nm CSSA	0.9835	0.5898	0.8208±0.0754	0.8225
440 nm Real part	1.6000	1.3300	1.4423±0.0638	1.4374
440 nm Imaginary part	0.0301	0.0005	0.0084±0.0047	0.0078

AOD: Aerosol optical depth
FAOD: Fine aerosol optical depth
CAOD: Coarse aerosol optical depth
SAOD: Scattering aerosol optical depth
FSAOD: Scattering aerosol optical depth in fine mode
CSAOD: Scattering aerosol optical depth in coarse mode
AAOD: Absorbing aerosol optical depth
FAAOD: Absorbing aerosol optical depth in fine mode
CAAOD: Absorbing aerosol optical depth in coarse mode
AE: Ångström exponent of total aerosols
FAE: Ångström exponent of fine aerosols
CAE: Ångström exponent of coarse aerosols
SAE: Ångström exponent of scattering aerosols
FSAE: Ångström exponent of scattering aerosols in fine mode
CSAE: Ångström exponent of scattering aerosols in coarse mode
AAE: Ångström exponent of absorbing aerosols
FAAE: Ångström exponent of absorbing aerosols in fine mode
CAAE: Ångström exponent of absorbing aerosols in coarse mode
SSA: Single scattering albedo of total aerosols
FSSA: Single scattering albedo of fine aerosols
CSSA: Single scattering albedo of coarse aerosols

1127

1128 Table 2 Seasonal mean±SD of the columnar aerosol optical properties in urban area of Nanjing

Factors	MAM	JJA	SON	DJF
550 nm AOD	0.6788±0.2919	0.7508±0.3749	0.5866±0.2447	0.6560±0.2976
550 nm FAOD	0.4739±0.2613	0.6798±0.3793	0.5149±0.2462	0.5687±0.2978
550 nm CAOD	0.2048±0.1356	0.0710±0.0599	0.0717±0.0346	0.0873±0.0685
550 nm SAOD	0.6284±0.2835	0.7031±0.3728	0.5495±0.2342	0.6157±0.2829
550 nm FSAOD	0.4529±0.2552	0.6463±0.3760	0.4901±0.2366	0.5428±0.2846
550 nm CSAOD	0.1756±0.1225	0.0568±0.0497	0.0593±0.0315	0.0728±0.0601
550 nm AAOD	0.0503±0.0208	0.0477±0.0307	0.0372±0.0200	0.0403±0.0271
550 nm FAAOD	0.0211±0.0125	0.0335±0.0212	0.0248±0.0157	0.0259±0.0211
550 nm CAAOD	0.0292±0.0165	0.0142±0.0137	0.0124±0.0066	0.0144±0.0111
440/870 nm AE	0.9915±0.2385	1.2174±0.2639	1.3744±0.1907	1.3134±0.2461
440/870 nm FAE	1.7474±0.2896	1.4701±0.3075	1.7408±0.2582	1.6935±0.3019
440/870 nm CAE	-0.1998±0.0352	-0.1699±0.0471	-0.1862±0.0424	-0.1807±0.0464
440/870 nm SAE	0.9812±0.2687	1.2733±0.2950	1.3824±0.2043	1.2956±0.2697
440/870 nm SFAE	1.7555±0.2862	1.5218±0.3397	1.7492±0.2545	1.6809±0.3039
440/870 nm SCAE	-0.3752±0.0743	-0.2815±0.0678	-0.3797±0.0991	-0.4016±0.1162
440/870 nm AAE	1.1885±0.4500	0.7971±0.2657	1.3290±0.4533	1.5007±0.4520
440/870 nm FAAE	1.7352±0.6059	0.9943±0.2672	1.6715±0.5970	1.8947±0.6545
440/870 nm CAAE	0.8542±0.4665	0.3771±0.2753	0.8312±0.4479	0.9798±0.4235
550 nm SSA	0.9204±0.0313	0.9241±0.0422	0.9348±0.0331	0.9378±0.0331
550 nm FSSA	0.9527±0.0237	0.9405±0.0356	0.9518±0.0253	0.9555±0.0265
550 nm CSSA	0.8340±0.0628	0.7868±0.0953	0.8115±0.0752	0.8211±0.0810
440 nm Real part	1.4647±0.0628	1.4075±0.0609	1.4252±0.0602	1.4404±0.0582
440 nm Imaginary part	0.0084±0.0040	0.0083±0.0052	0.0080±0.0044	0.0083±0.0053

1129

1130 Table 3. The annual mean aerosol direct radiative forcing (W/m^2) in urban area of Nanjing

Species	Clear sky	
	TOA	Surface
TA	-10.69±3.37	-25.54±2.83
FA	-11.17±3.09	-21.37±2.78
CA	-0.33±0.60	-6.15±2.90
SA	-16.45±2.81	-17.17±2.96
FSA	-15.08±3.18	-15.74±3.35
CSA	-2.31±1.18	-2.42±1.24
AA	5. 76±1.27	-8.38±1.56
FAA	3.91±0.95	-5.63±1.16
CAA	1.99±1.07	-3.73±1.71

1131 TA: Total aerosols

1132 FA: Fine aerosols

1133 CA: Coarse aerosols

1134 SA: All scattering aerosols

1135 FSA: Scattering aerosols in fine mode

CSA: Scattering aerosols in coarse mode

AA: All absorbing aerosols' forcing

FAA: Fine absorbing aerosols' forcing

CAA: Coarse absorbing aerosols' forcing

Figures:

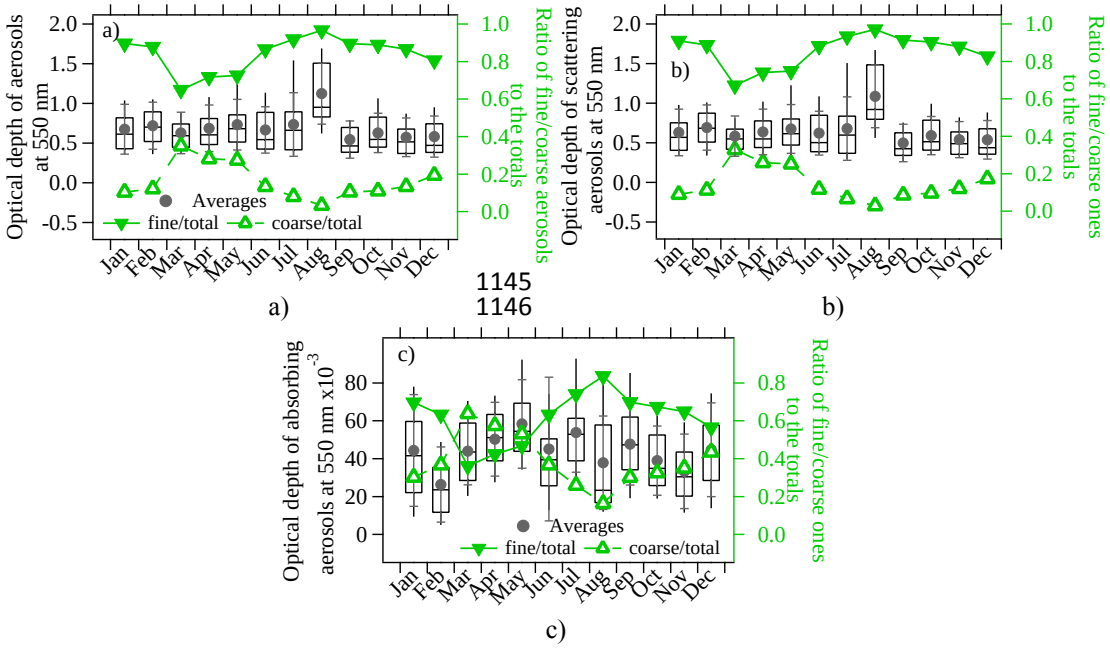

a) b) c)

Figure 1.

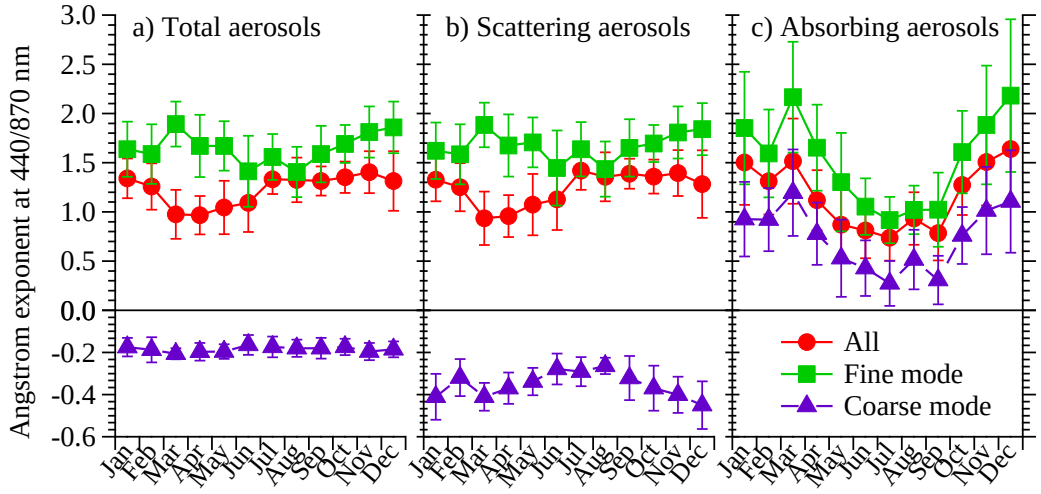

Figure 2.

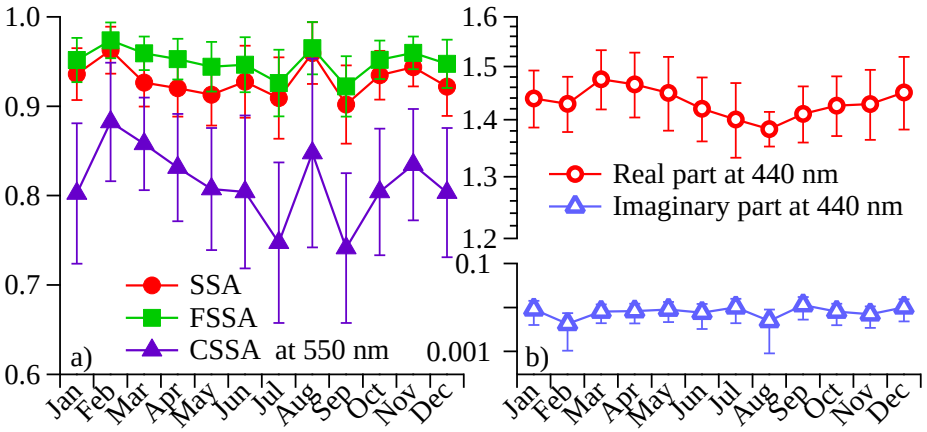

Figure 3

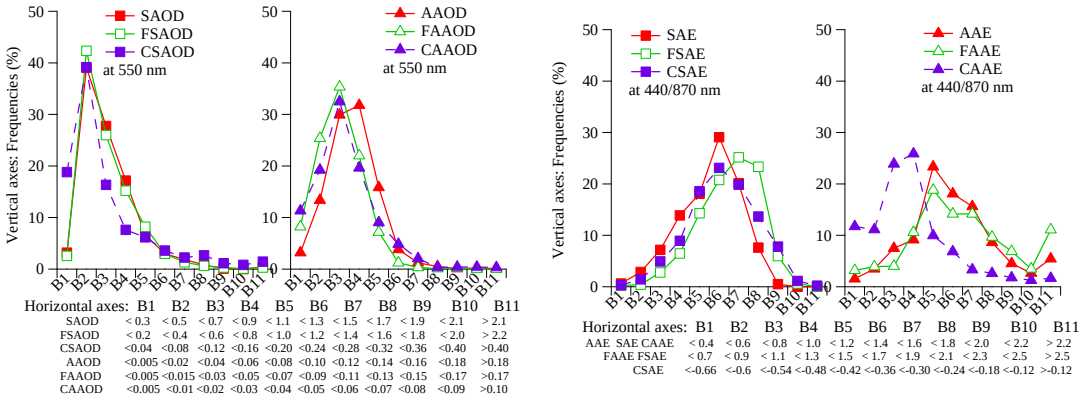

	B1	B2	B3	B4	B5	B6	B7	B8	B9	B10	B11
SAOD	< 0.3	< 0.5	< 0.7	< 0.9	< 1.1	< 1.3	< 1.5	< 1.7	< 1.9	< 2.1	> 2.1
FSAOD	< 0.2	< 0.4	< 0.6	< 0.8	< 1.0	< 1.2	< 1.4	< 1.6	< 1.8	< 2.0	> 2.2
CSAOD	<0.04	<0.08	<0.12	<0.16	<0.20	<0.24	<0.28	<0.32	<0.36	<0.40	>0.40
AAOD	<0.005	<0.02	<0.04	<0.06	<0.08	<0.10	<0.12	<0.14	<0.16	<0.18	>0.18
FAAOD	<0.005	<0.015	<0.03	<0.05	<0.07	<0.09	<0.11	<0.13	<0.15	<0.17	>0.17
CAAOD	<0.005	<0.01	<0.02	<0.03	<0.04	<0.05	<0.06	<0.07	<0.08	<0.09	>0.10

a)

	B1	B2	B3	B4	B5	B6	B7	B8	B9	B10	B11
AAE	< 0.4	< 0.6	< 0.8	< 1.0	< 1.2	< 1.4	< 1.6	< 1.8	< 2.0	< 2.2	> 2.2
SAE CAAE	< 0.4	< 0.6	< 0.8	< 1.0	< 1.2	< 1.4	< 1.6	< 1.8	< 2.0	< 2.2	> 2.2
FAAE FSAE	< 0.7	< 0.9	< 1.1	< 1.3	< 1.5	< 1.7	< 1.9	< 2.1	< 2.3	< 2.5	> 2.5
CSAE	<-0.66	<-0.6	<-0.54	<-0.48	<-0.42	<-0.36	<-0.30	<-0.24	<-0.18	<-0.12	>-0.12

b)

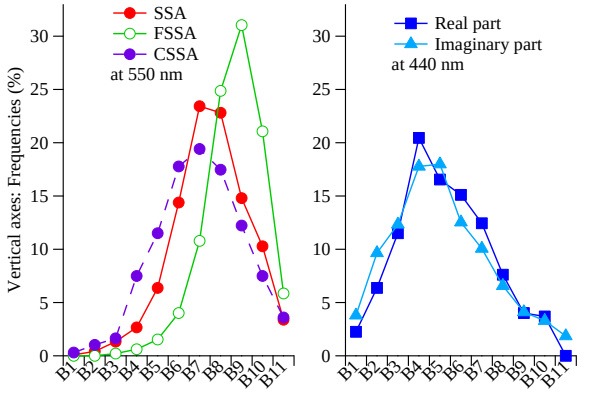

	B1	B2	B3	B4	B5	B6	B7	B8	B9	B10	B11
SSA FSSA	<0.81	<0.83	<0.85	<0.87	<0.89	<0.91	<0.93	<0.95	<0.97	<0.99	>0.99
CSSA	<0.60	<0.64	<0.68	<0.72	<0.76	<0.80	<0.84	<0.88	<0.92	<0.96	>0.96
Real	<1.33	<1.36	<1.39	<1.42	<1.46	<1.50	<1.54	<1.58	<1.62	<1.66	>1.66
Imag	<0.001	<0.003	<0.005	<0.007	<0.009	<0.011	<0.013	<0.015	<0.017	<0.019	>0.019

c)

Figure 4

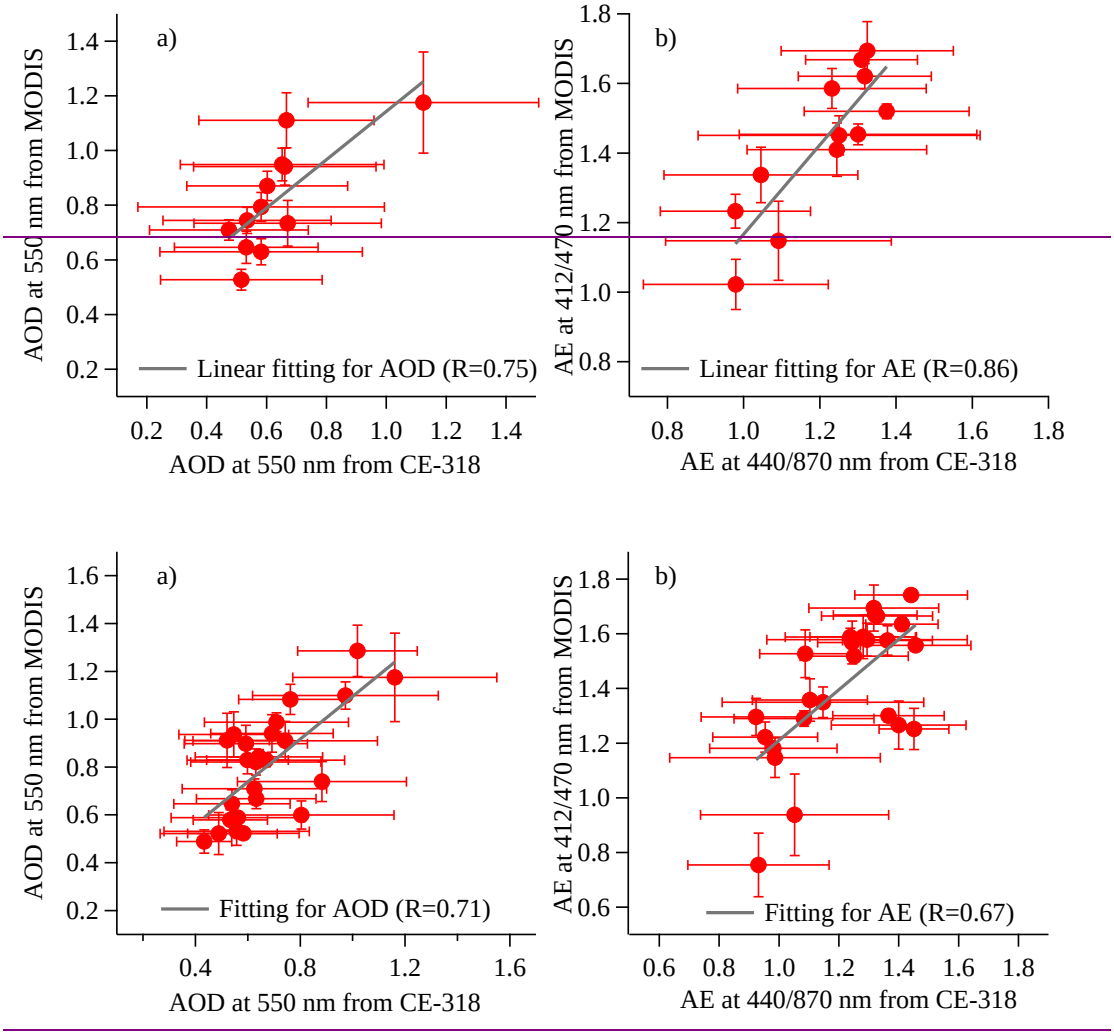

Figure 5

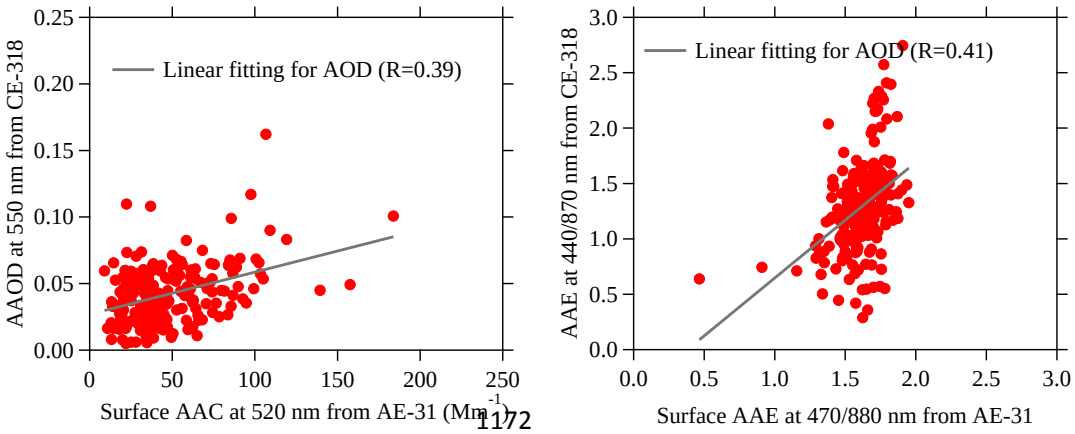

a) b)

Figure 6

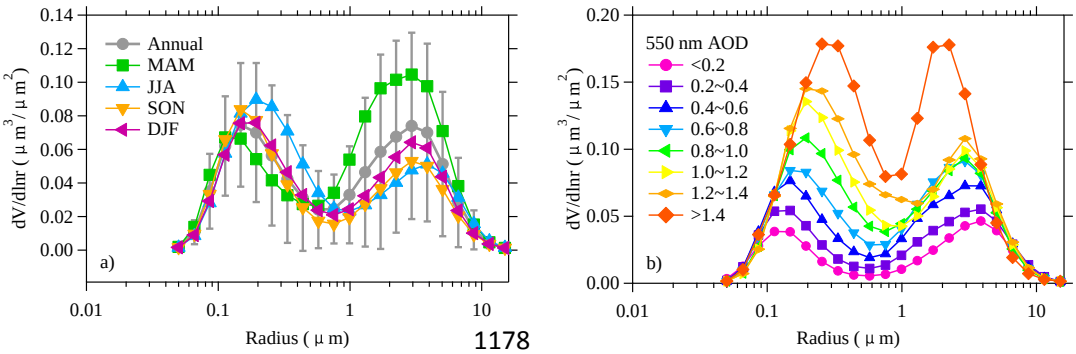

a) b)

Figure 7

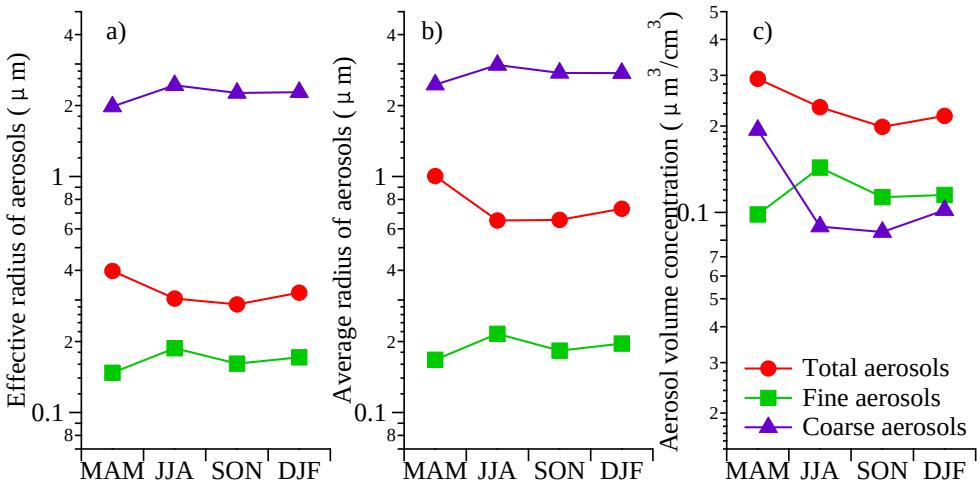

Horizontal axes: seasons

Figure 8

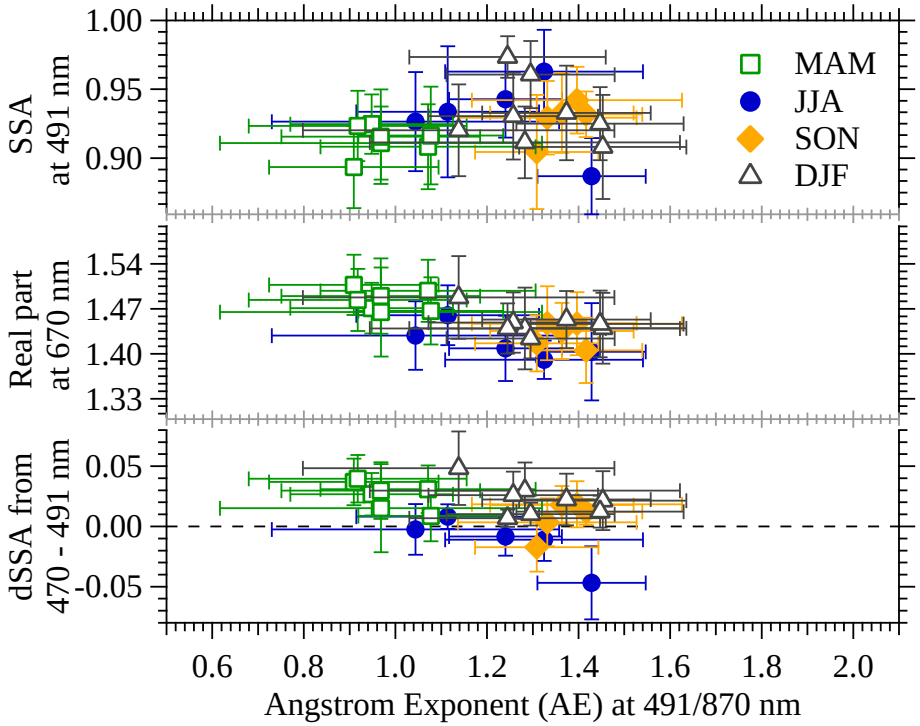

Figure 9

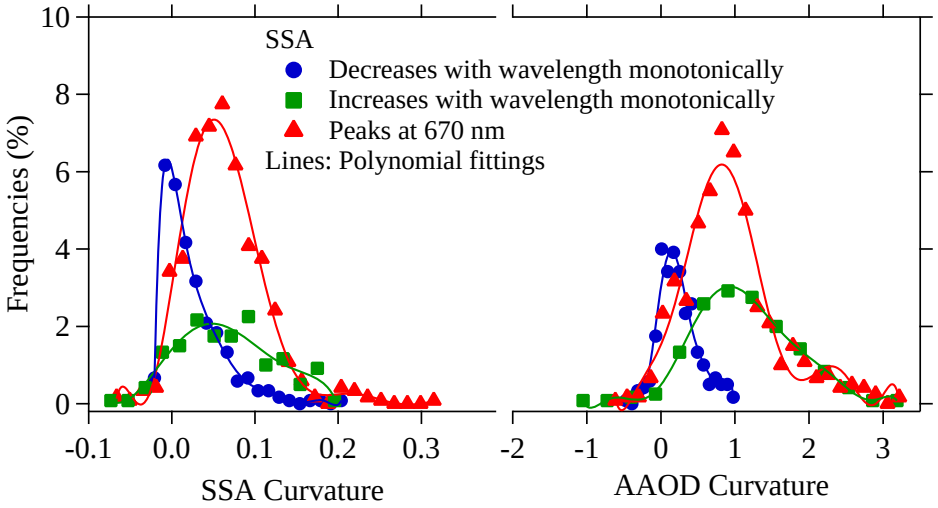

Figure 10

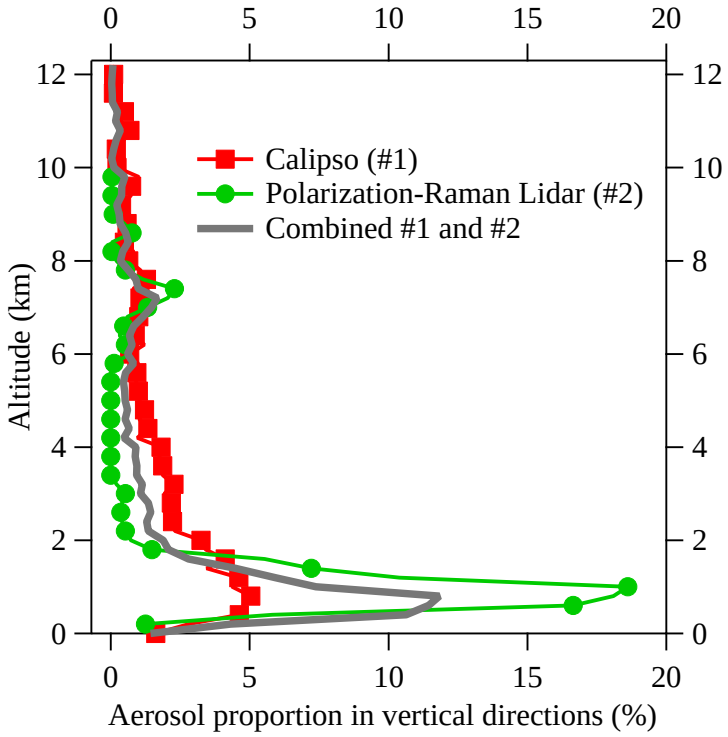

1191

1192 Figure 11

1193

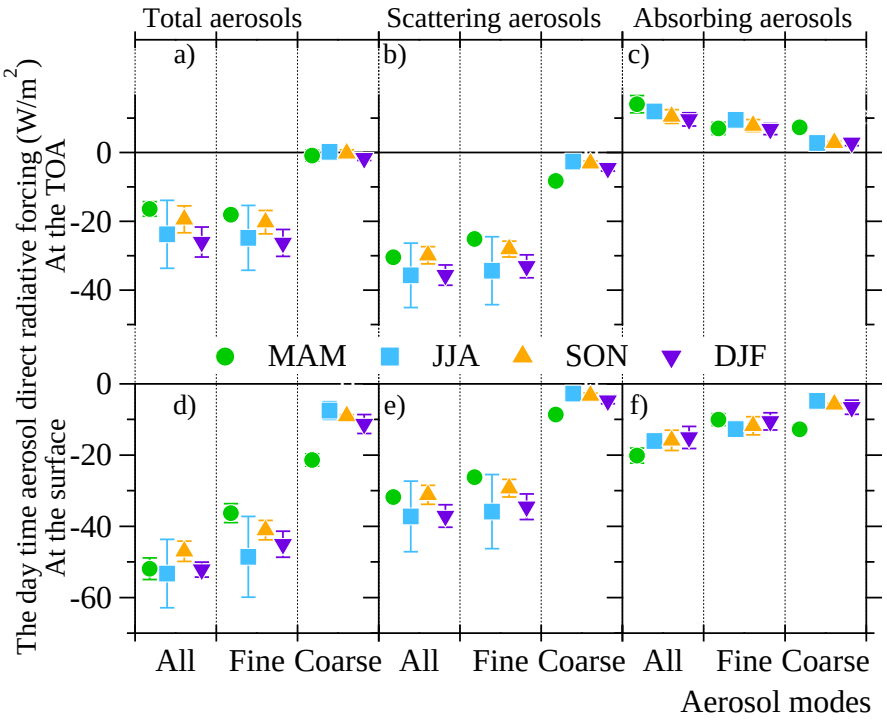

1194

1195 Figure 12

1196

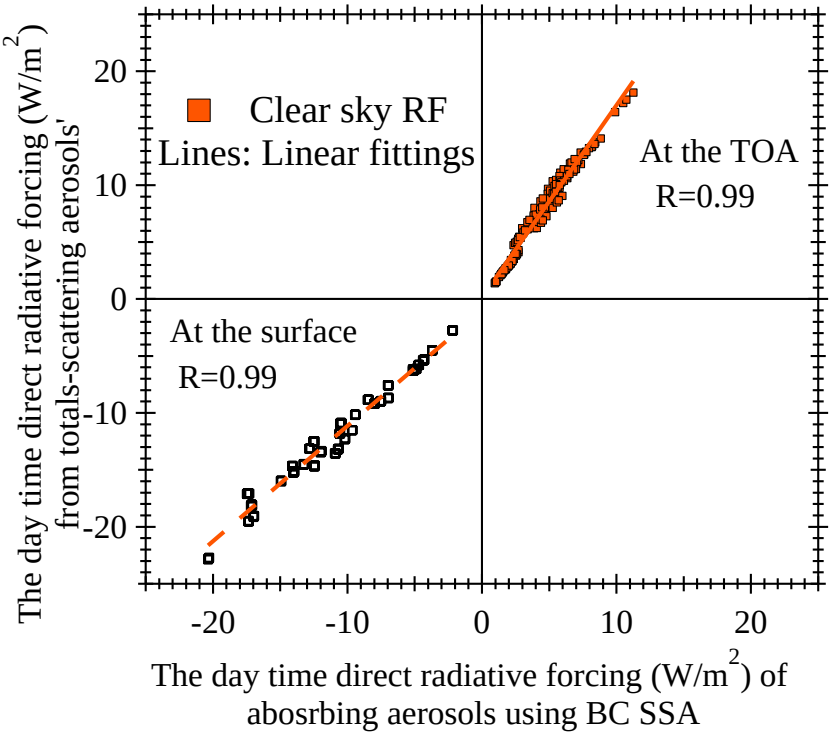

Figure 13

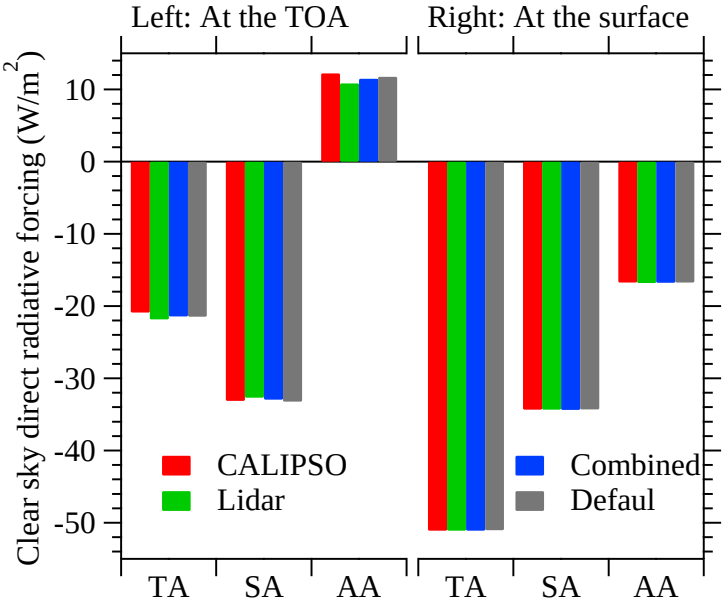

Figure 14